US 20250257526A1

(19) **United States**

(12) **Patent Application Publication** (10) **Pub. No.: US 2025/0257526 A1**

Fu et al. (43) **Pub. Date: Aug. 14, 2025**

(54) **PROCESS FOR PRODUCTION OF LIGNIN, ORGANIC ACIDS, ORGANIC CHEMICALS, PURE CO2, AND WATER FROM KRAFT BLACK LIQUOR WITH OPERATIONAL EFFICIENCIES**

(71) Applicant: **Georgia Tech Research Corporation**, Atlanta, GA (US)

(72) Inventors: **Qiang Fu**, Atlanta, GA (US); **Opeyemi Ojelade**, Atlanta, GA (US); **Quyen Tran**, Atlanta, GA (US); **Marco Avendano**, Atlanta, GA (US); **Scott Sinquefield**, Atlanta, GA (US); **Meisha Shofner**, Atlanta, GA (US); **Christopher W. Jones**, Atlanta, GA (US); **Sankar Nair**, Atlanta, GA (US)

(21) Appl. No.: **19/054,341**

(22) Filed: **Feb. 14, 2025**

Related U.S. Application Data

(60) Provisional application No. 63/553,482, filed on Feb. 14, 2024.

Publication Classification

(51) **Int. Cl.**
D21C 11/00 (2006.01)

(52) **U.S. Cl.**
CPC ***D21C 11/0007*** (2013.01); ***D21C 11/0014*** (2013.01); ***D21C 11/0042*** (2013.01)

(57) **ABSTRACT**

An exemplary embodiment of the present disclosure provides a process for generating new products from a kraft mill and improving operational efficiency of a kraft mill through extraction of bioderived organic acids and liquid CO2 from weak black liquor generated during a kraft process, comprising the steps of: filtering a weak black liquor (BL) stream generated in the kraft process downstream from a brownstock washer to remove a first portion of lignin and generate a reduced lignin or de-lignified permeate and a retentate; removing the reduced lignin or de-lignified permeate from the kraft process; processing at least the de-lignified permeate to generate organic acids, liquid CO2, water, and raffinate containing salts; recovering the organic acids and liquid CO2; and returning the raffinate containing salts to the kraft process downstream of a recovery boiler.

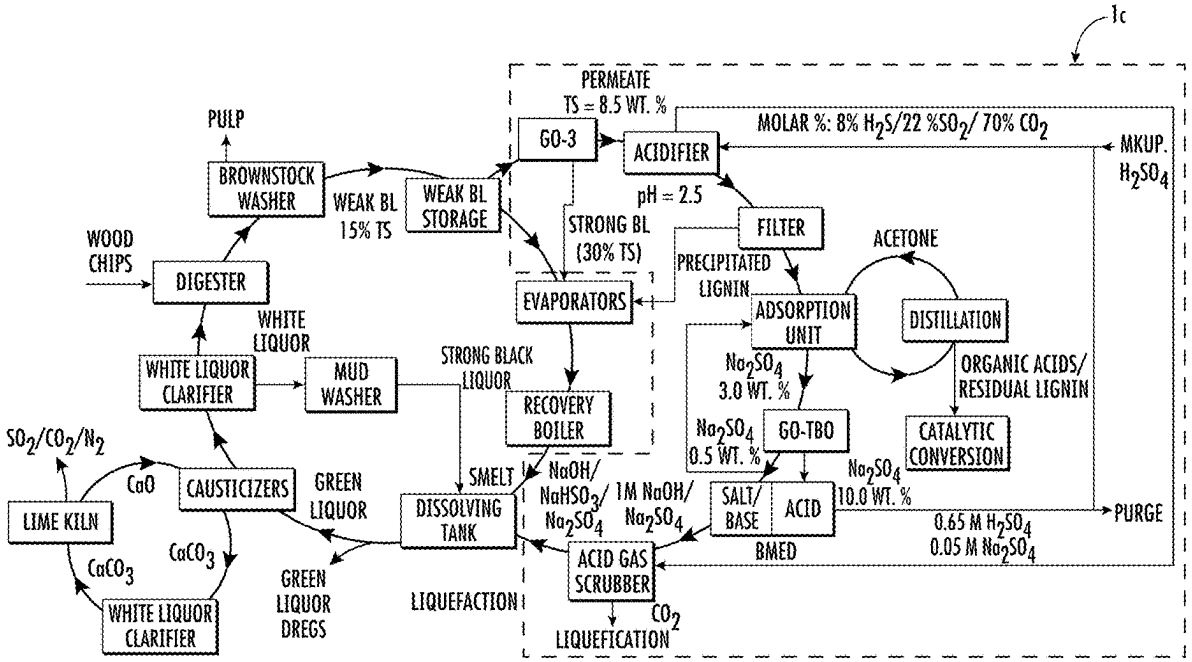

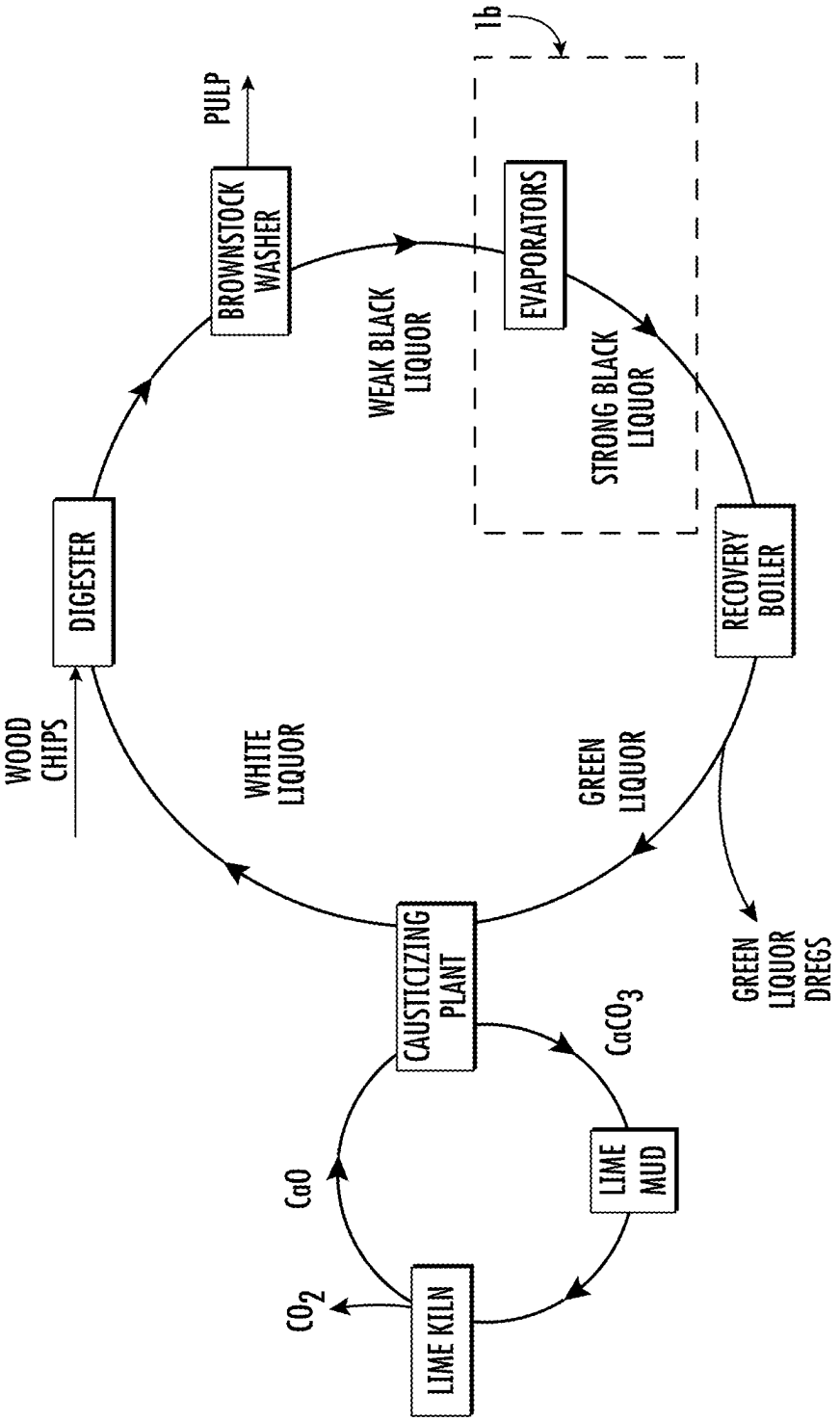
1b
PULP
BROWNSTOCK WASHER
EVAPORATORS
WEAK BLACK LIQUOR
STRONG BLACK LIQUOR
DIGESTER
RECOVERY BOILER
WOOD CHIPS
WHITE LIQUOR
GREEN LIQUOR
CAUSTICIZING PLANT
GREEN LIQUOR DREGS
$CaCO_3$
LIME MUD
CaO
CO_2
LIME KILN

FIG. 1A

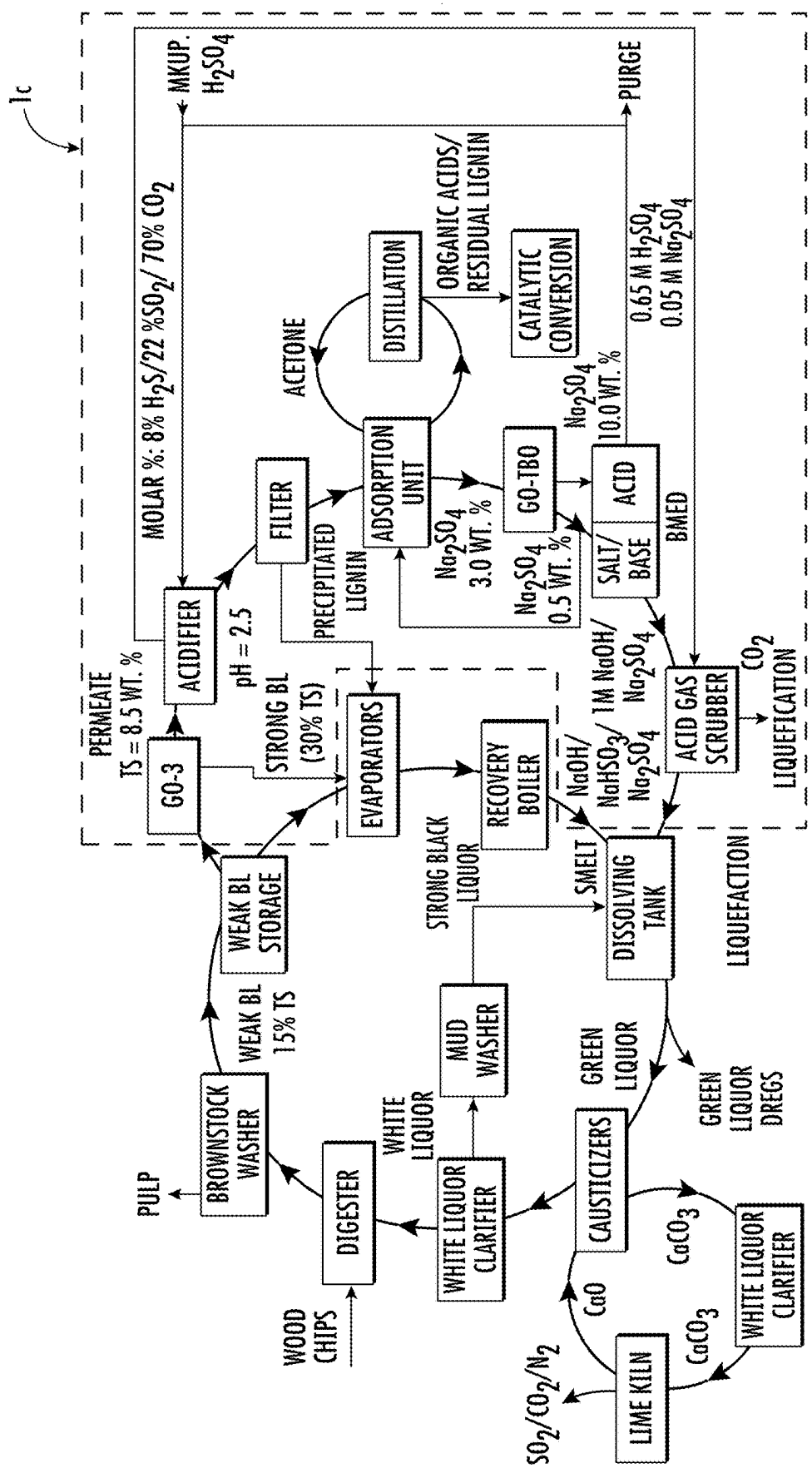
1c
MKUP. H_2SO_4
PURGE
MOLAR %: 8% H_2S/22 % SO_2/ 70% CO_2
ORGANIC ACIDS/ RESIDUAL LIGNIN
DISTILLATION
CATALYTIC CONVERSION
ACETONE
0.65 M H_2SO_4
0.05 M Na_2SO_4
Na_2SO_4 10.0 WT. %
FILTER
ADSORPTION UNIT
GO-TBO
ACID
SALT/ BASE
BMED
PRECIPITATED LIGNIN
Na_2SO_4 3.0 WT. %
Na_2SO_4 0.5 WT. %
PERMEATE TS = 8.5 WT. %
ACIDIFIER
pH = 2.5
GO-3
STRONG BL (30% TS)
EVAPORATORS
RECOVERY BOILER
NaOH/ $NaHSO_3$/ Na_2SO_4
1M NaOH/ Na_2SO_4
ACID GAS SCRUBBER
CO_2
LIQUEFICATION
WEAK BL STORAGE
STRONG BLACK LIQUOR
SMELT
DISSOLVING TANK
LIQUEFACTION
WEAK BL 15% TS
MUD WASHER
GREEN LIQUOR
GREEN LIQUOR DREGS
BROWNSTOCK WASHER
WHITE LIQUOR
CAUSTICIZERS
PULP
DIGESTER
WHITE LIQUOR CLARIFIER
CaO
$CaCO_3$
WHITE LIQUOR CLARIFIER
WOOD CHIPS
LIME KILN
$SO_2/CO_2/N_2$
$CaCO_3$

FIG. 1B

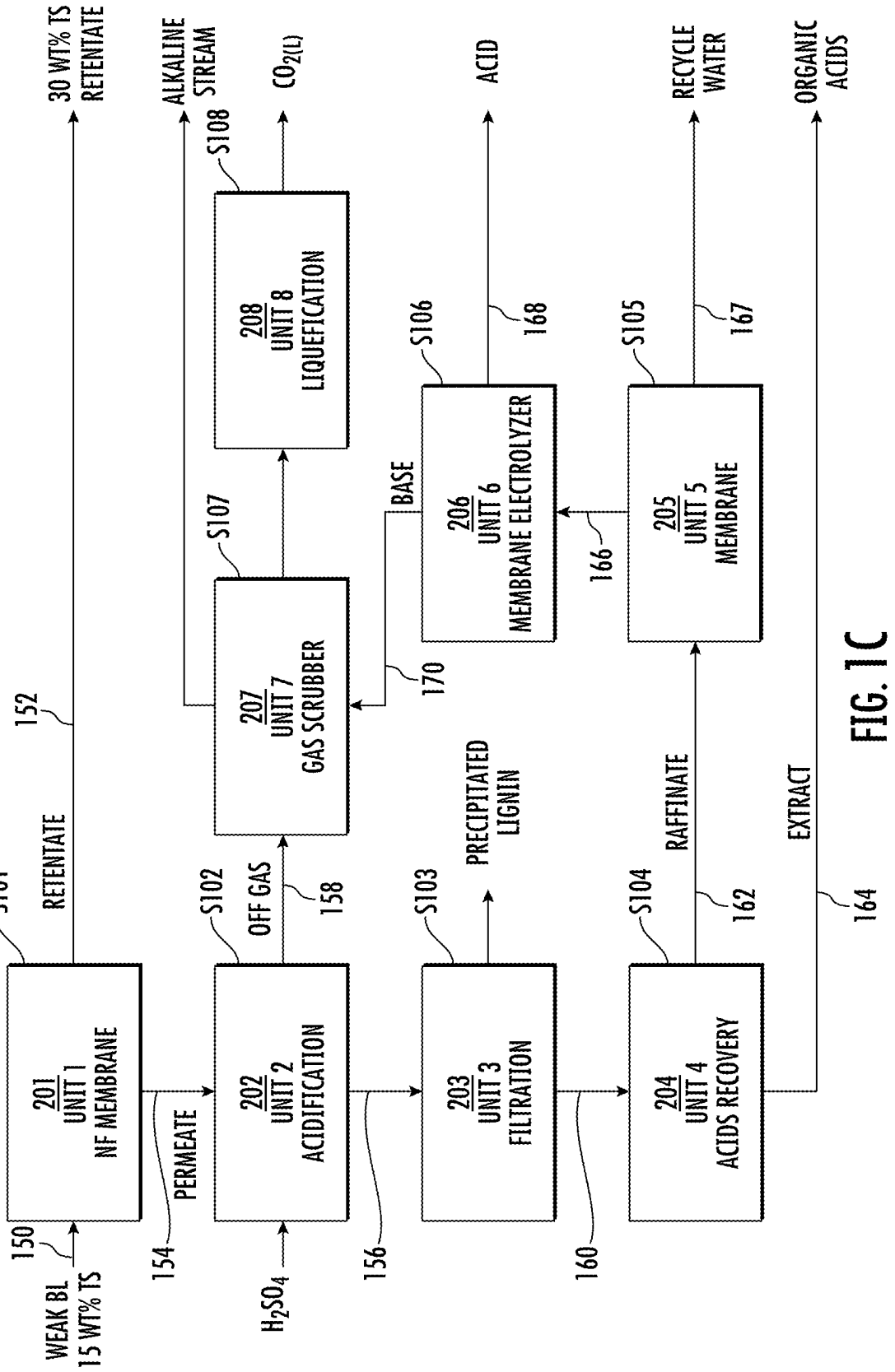
WEAK BL
15 WT% TS
150
201
UNIT 1
NF MEMBRANE
S101
RETENTATE
152
30 WT% TS
RETENTATE
PERMEATE
154
202
UNIT 2
ACIDIFICATION
S102
OFF GAS
158
207
UNIT 7
GAS SCRUBBER
S107
ALKALINE
STREAM
208
UNIT 8
LIQUEFICATION
S108
$CO_{2(L)}$
H_2SO_4
156
203
UNIT 3
FILTRATION
S103
PRECIPITATED
LIGNIN
BASE
170
206
UNIT 6
MEMBRANE ELECTROLYZER
S106
ACID
168
160
204
UNIT 4
ACIDS RECOVERY
S104
RAFFINATE
162
166
205
UNIT 5
MEMBRANE
S105
RECYCLE
WATER
167
EXTRACT
164
ORGANIC
ACIDS

FIG. 1C

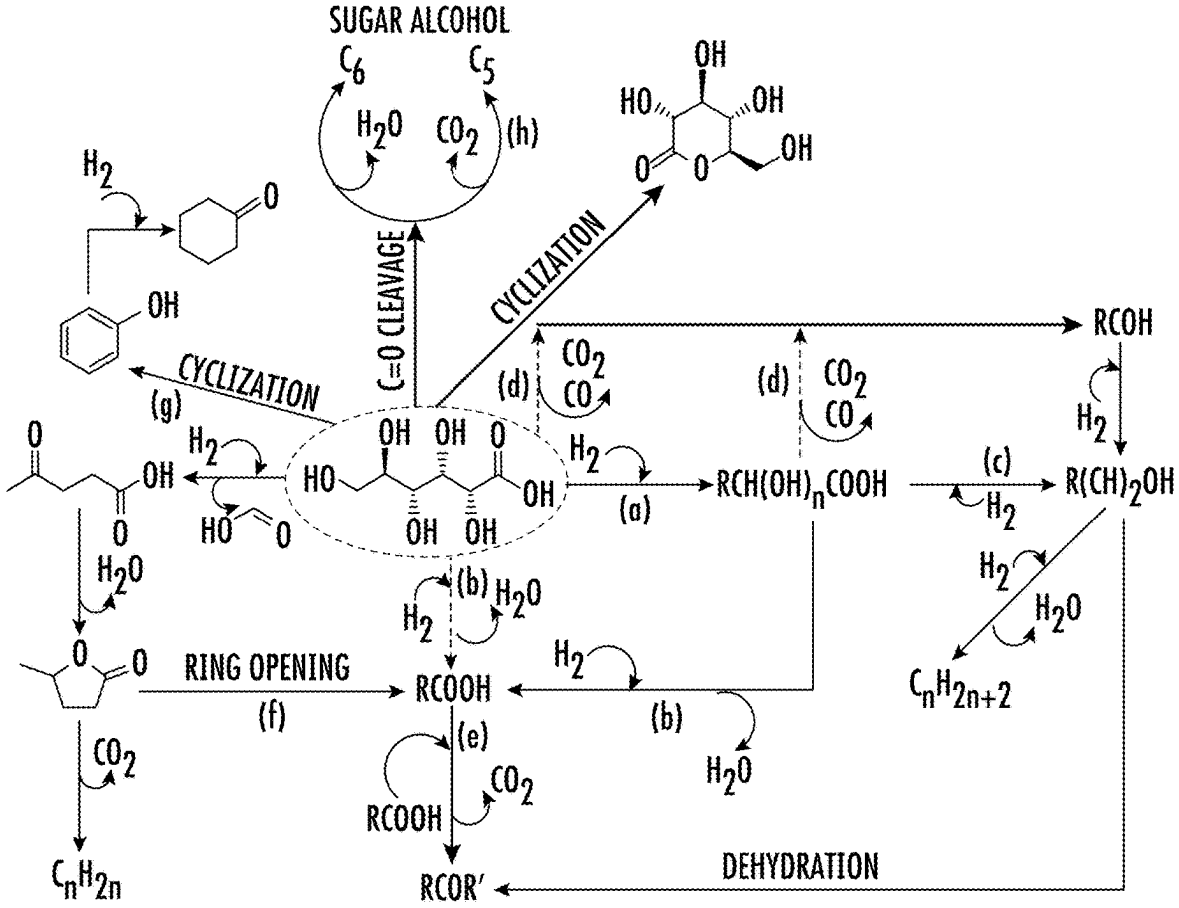
SUGAR ALCOHOL
C6
C5
H2O
CO2
(h)
C=O CLEAVAGE
CYCLIZATION
CYCLIZATION
(g)
RCOH
(d)
CO2
CO
(d)
CO2
CO
H2
(a)
RCH(OH)nCOOH
(c)
R(CH)2OH
H2O
(b)
RING OPENING
(f)
RCOOH
(e)
CO2
RCOOH
(b)
H2O
CnH2n
CnH2n+2
RCOR'
DEHYDRATION

FIG. 2

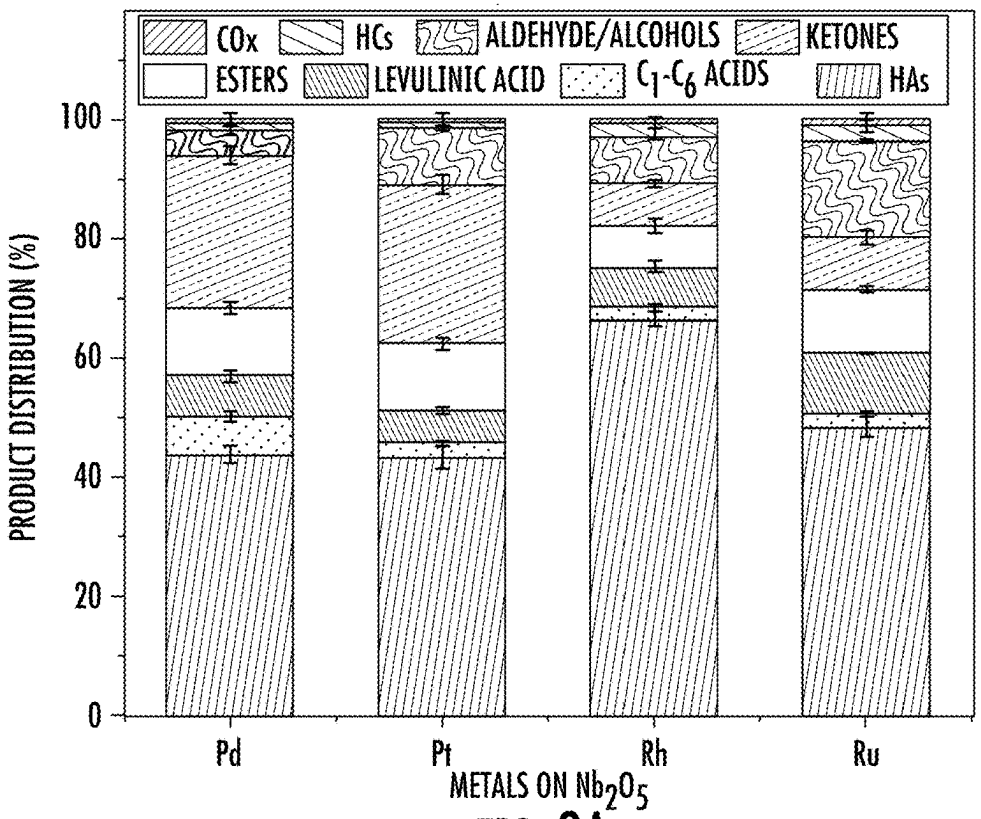
COx
HCs
ALDEHYDE/ALCOHOLS
KETONES
ESTERS
LEVULINIC ACID
C_1-C_6 ACIDS
HAs
PRODUCT DISTRIBUTION (%)
0
20
40
60
80
100
Pd
Pt
Rh
Ru
METALS ON Nb_2O_5

FIG. 3A

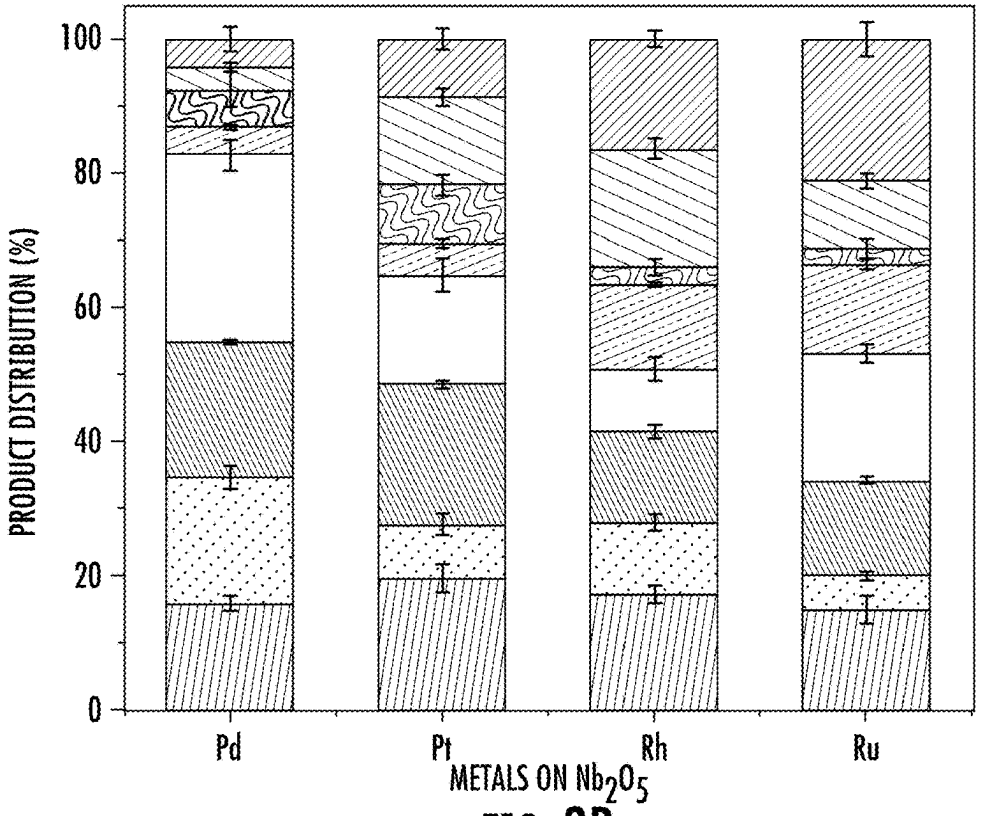
PRODUCT DISTRIBUTION (%)
0
20
40
60
80
100
Pd
Pt
Rh
Ru
METALS ON Nb_2O_5

FIG. 3B

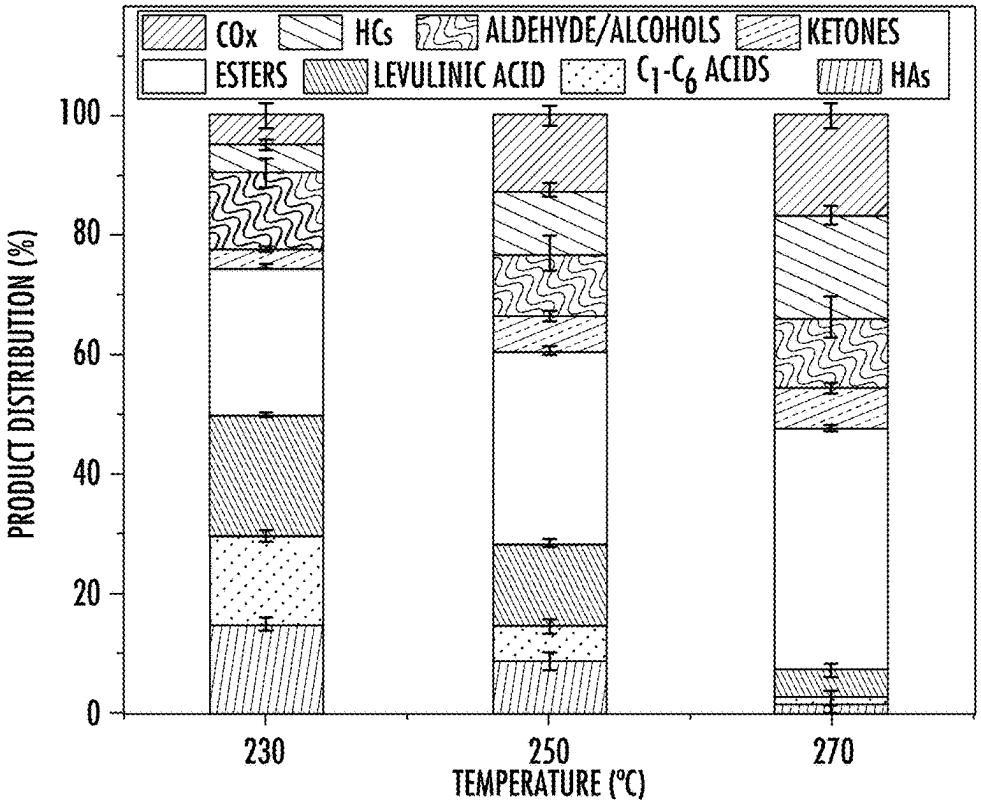
COx
HCs
ALDEHYDE/ALCOHOLS
KETONES
ESTERS
LEVULINIC ACID
C_1-C_6 ACIDS
HAs
PRODUCT DISTRIBUTION (%)
0
20
40
60
80
100
230
250
270
TEMPERATURE (°C)

FIG. 4A

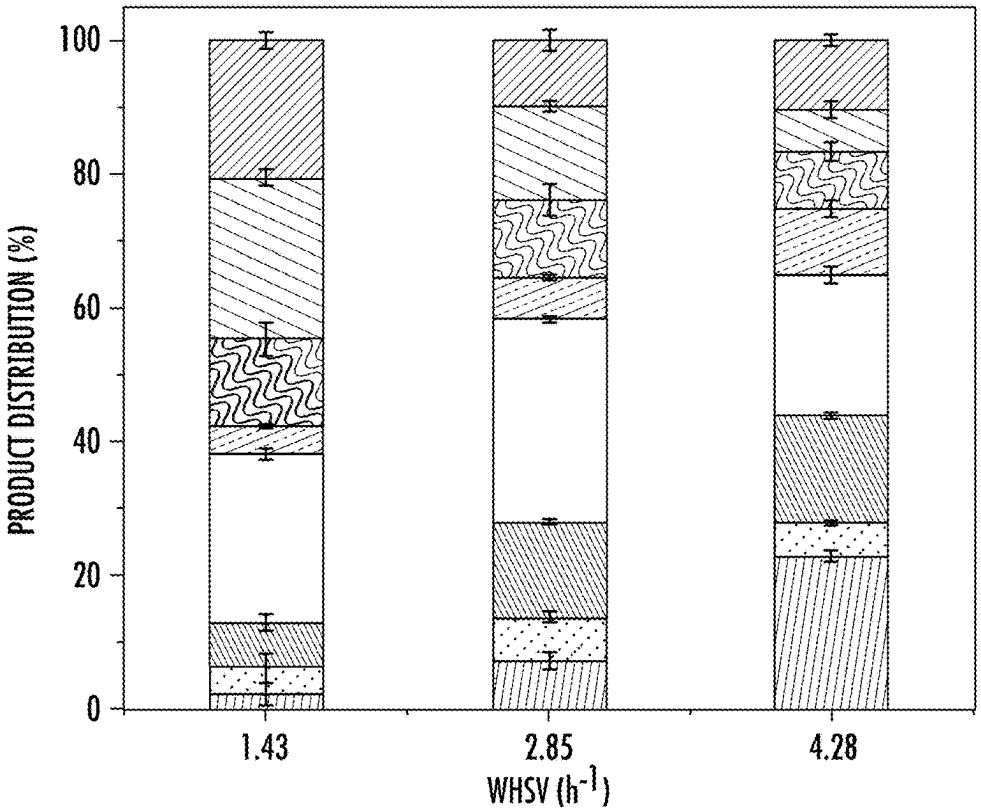
PRODUCT DISTRIBUTION (%)
0
20
40
60
80
100
1.43
2.85
4.28
WHSV (h^{-1})

FIG. 4B

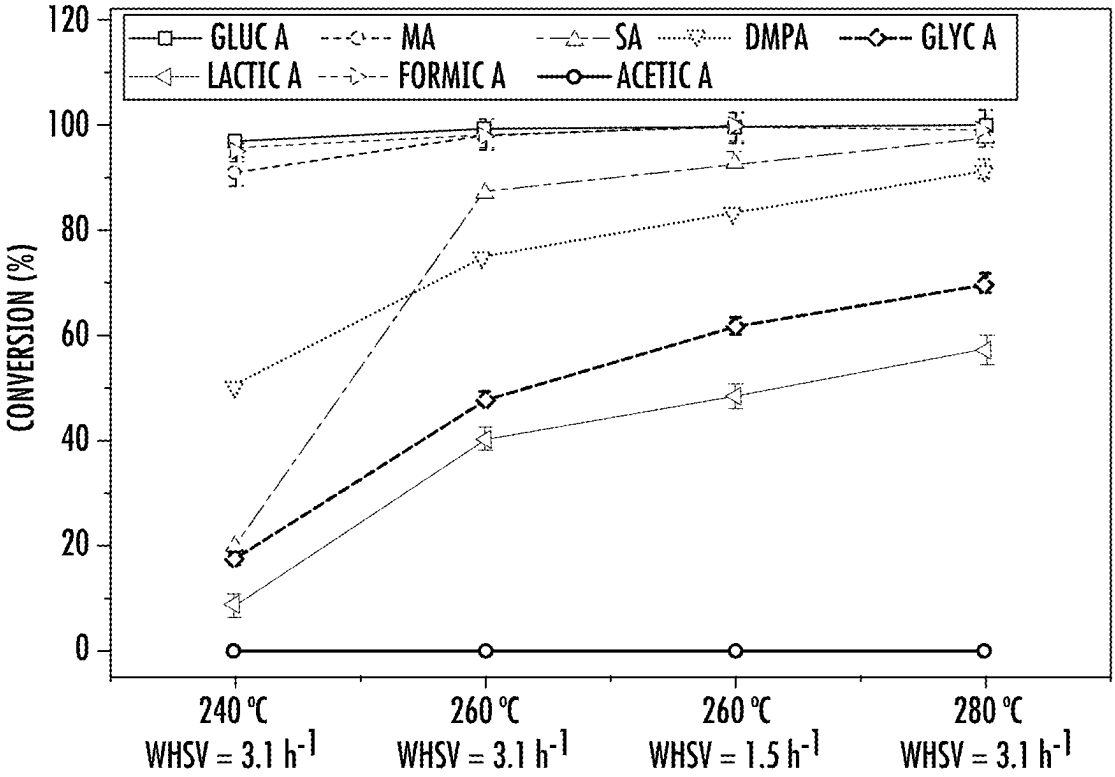
GLUC A
MA
SA
DMPA
GLYC A
LACTIC A
FORMIC A
ACETIC A
CONVERSION (%)
120
100
80
60
40
20
0
240 °C
WHSV = 3.1 h-1
260 °C
WHSV = 3.1 h-1
260 °C
WHSV = 1.5 h-1
280 °C
WHSV = 3.1 h-1

FIG. 5A

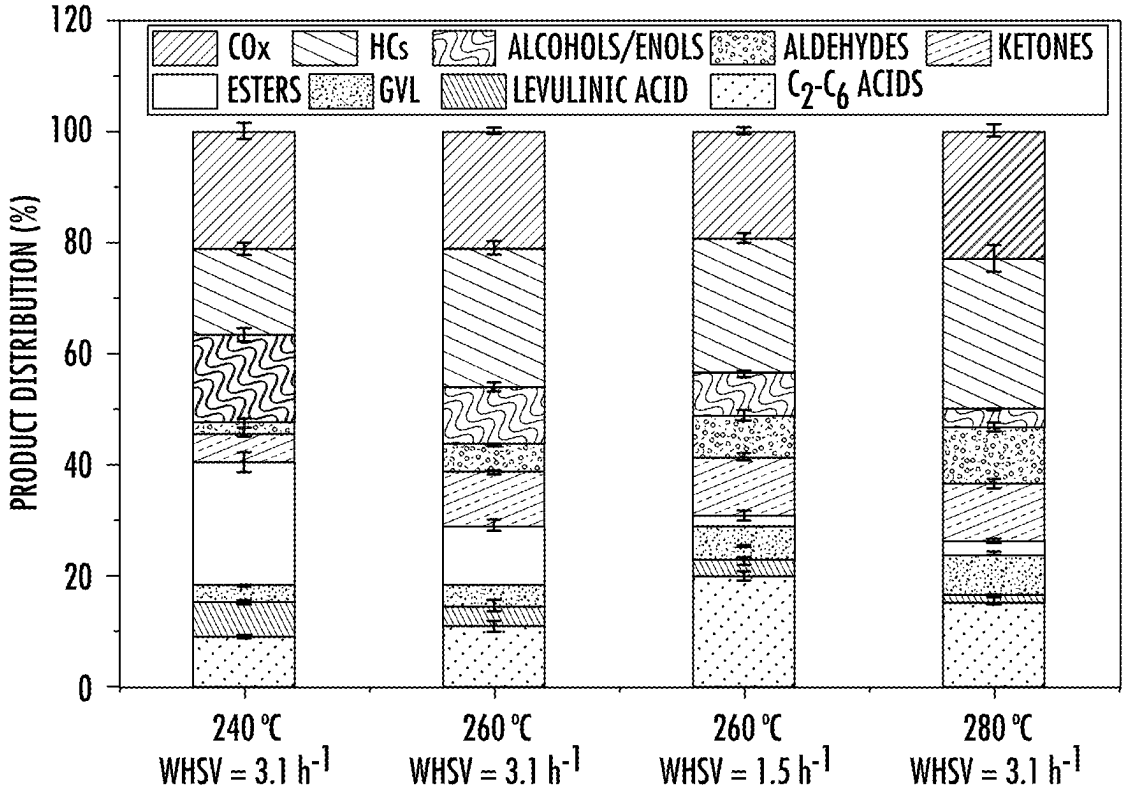
COx
HCs
ALCOHOLS/ENOLS
ALDEHYDES
KETONES
ESTERS
GVL
LEVULINIC ACID
C2-C6 ACIDS
PRODUCT DISTRIBUTION (%)
120
100
80
60
40
20
0
240 °C
WHSV = 3.1 h-1
260 °C
WHSV = 3.1 h-1
260 °C
WHSV = 1.5 h-1
280 °C
WHSV = 3.1 h-1

FIG. 5B

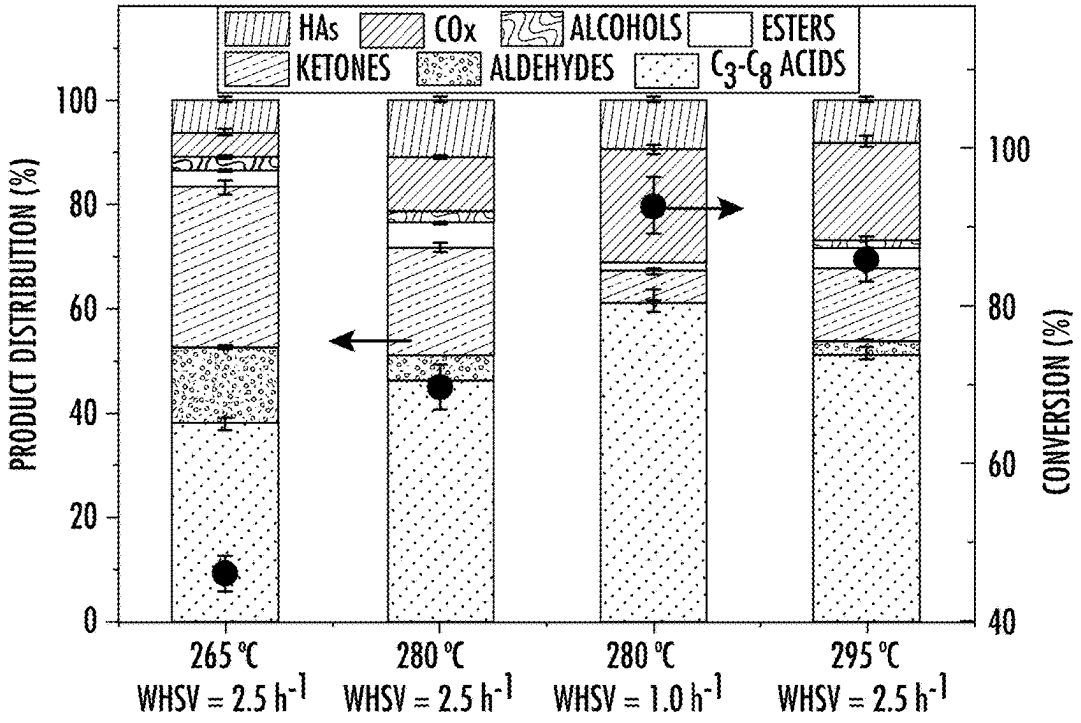
HAs
COx
ALCOHOLS
ESTERS
KETONES
ALDEHYDES
C3-C8 ACIDS
PRODUCT DISTRIBUTION (%)
CONVERSION (%)
0
20
40
60
80
100
265 °C
WHSV = 2.5 h-1
280 °C
WHSV = 2.5 h-1
280 °C
WHSV = 1.0 h-1
295 °C
WHSV = 2.5 h-1

FIG. 6A

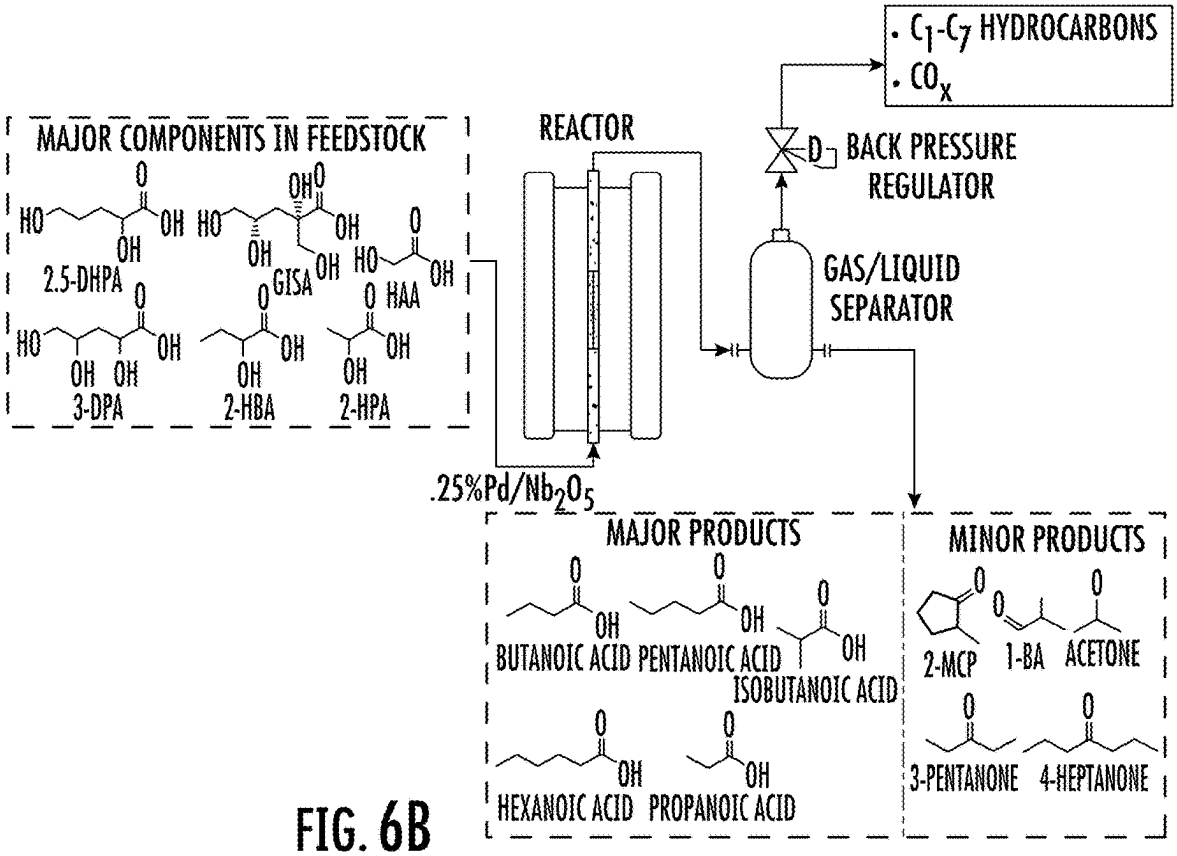
• C1-C7 HYDROCARBONS
• COx
MAJOR COMPONENTS IN FEEDSTOCK
2.5-DHPA
GISA
HAA
3-DPA
2-HBA
2-HPA
REACTOR
BACK PRESSURE REGULATOR
GAS/LIQUID SEPARATOR
.25%Pd/Nb2O5
MAJOR PRODUCTS
BUTANOIC ACID
PENTANOIC ACID
ISOBUTANOIC ACID
HEXANOIC ACID
PROPANOIC ACID
MINOR PRODUCTS
2-MCP
1-BA
ACETONE
3-PENTANONE
4-HEPTANONE

FIG. 6B

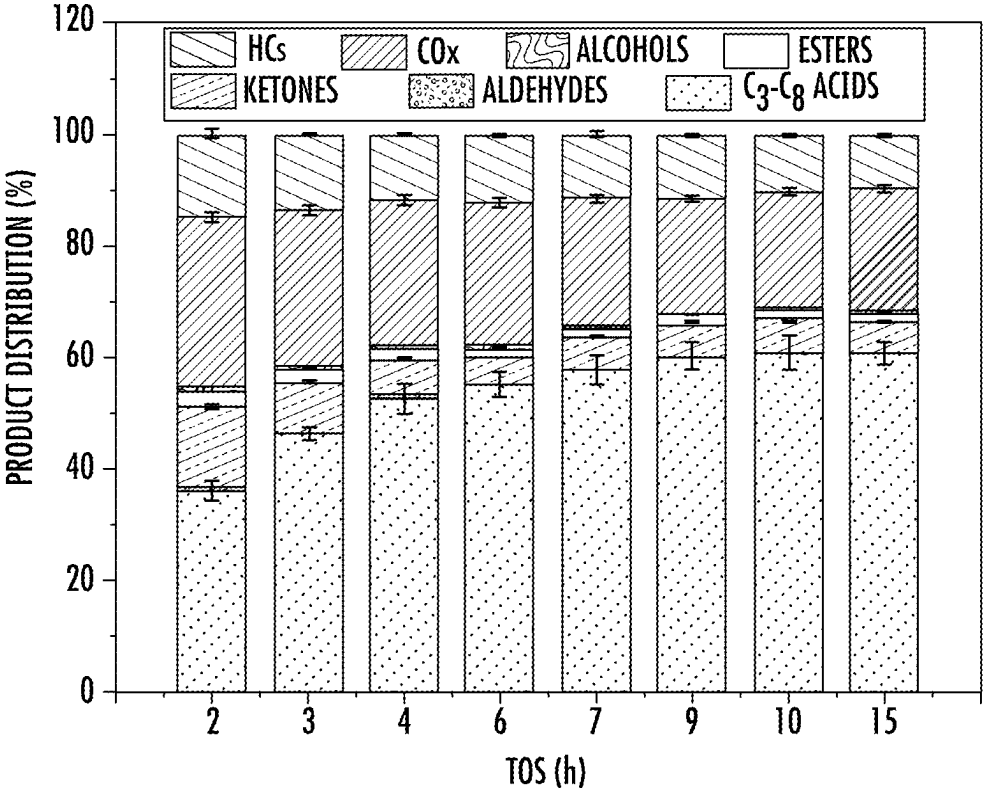
HCs
COx
ALCOHOLS
ESTERS
KETONES
ALDEHYDES
C3-C8 ACIDS
PRODUCT DISTRIBUTION (%)
TOS (h)

FIG. 7A

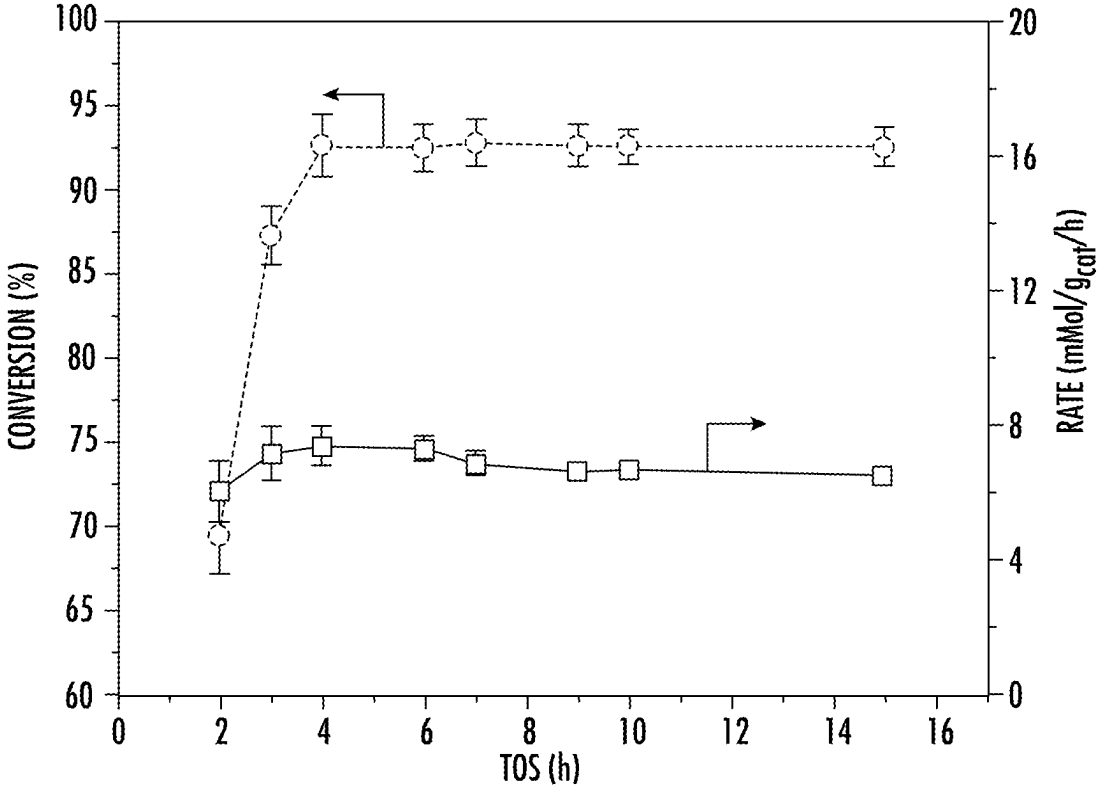
CONVERSION (%)
RATE (mMol/gcat/h)
TOS (h)

FIG. 7B

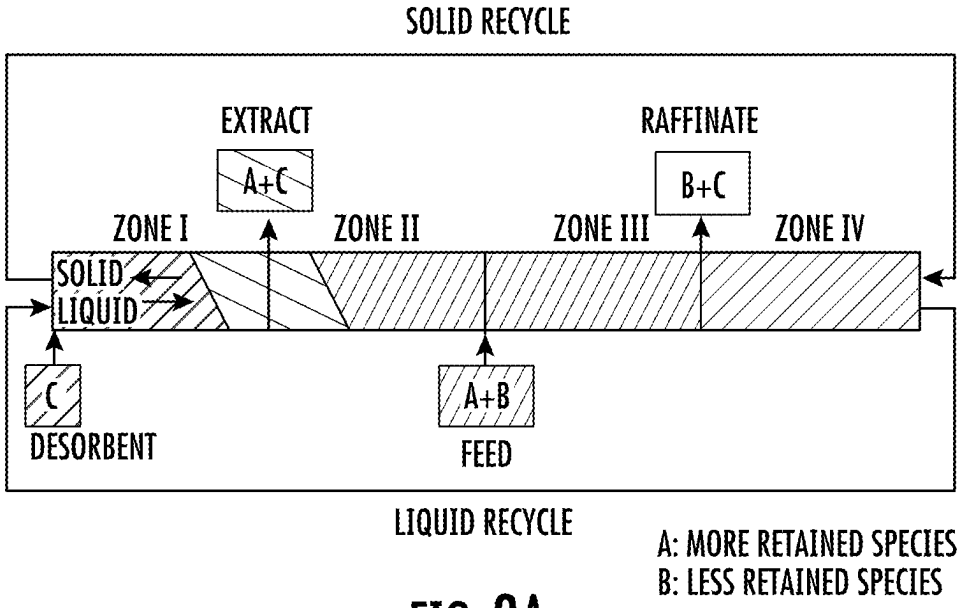
SOLID RECYCLE
EXTRACT
A+C
RAFFINATE
B+C
ZONE I
ZONE II
ZONE III
ZONE IV
SOLID
LIQUID
C
DESORBENT
A+B
FEED
LIQUID RECYCLE
A: MORE RETAINED SPECIES
B: LESS RETAINED SPECIES

FIG. 8A

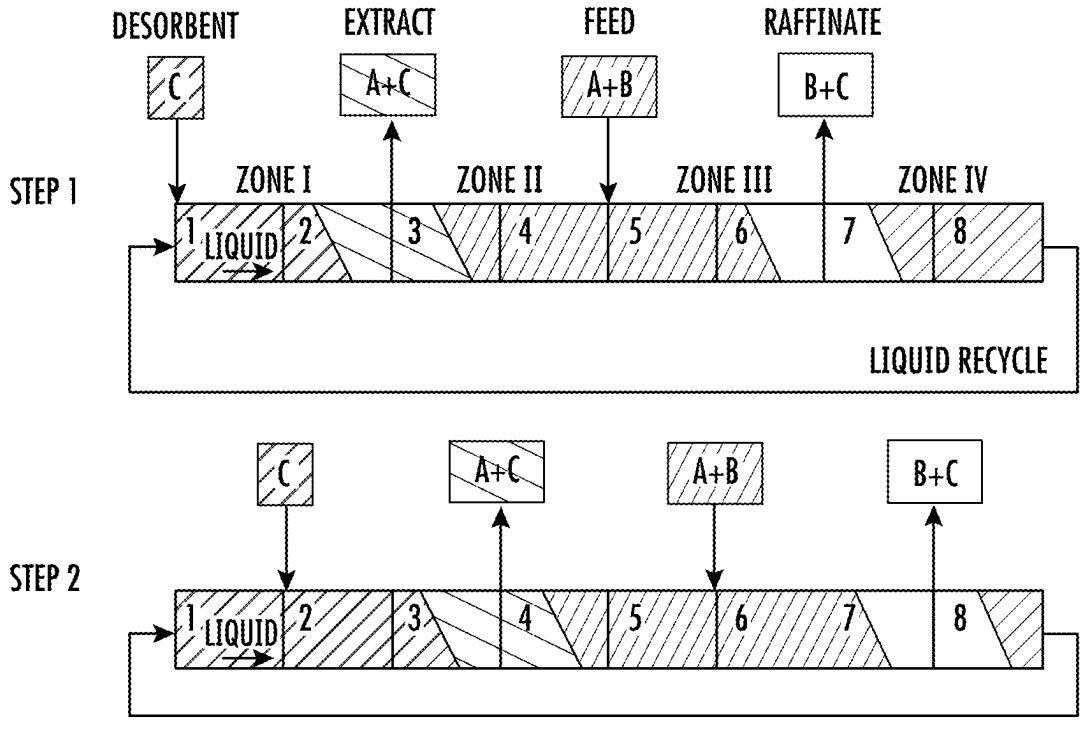
DESORBENT
EXTRACT
FEED
RAFFINATE
C
A+C
A+B
B+C
STEP 1
ZONE I
ZONE II
ZONE III
ZONE IV
1
LIQUID
2
3
4
5
6
7
8
LIQUID RECYCLE
C
A+C
A+B
B+C
STEP 2
1
LIQUID
2
3
4
5
6
7
8

FIG. 8B

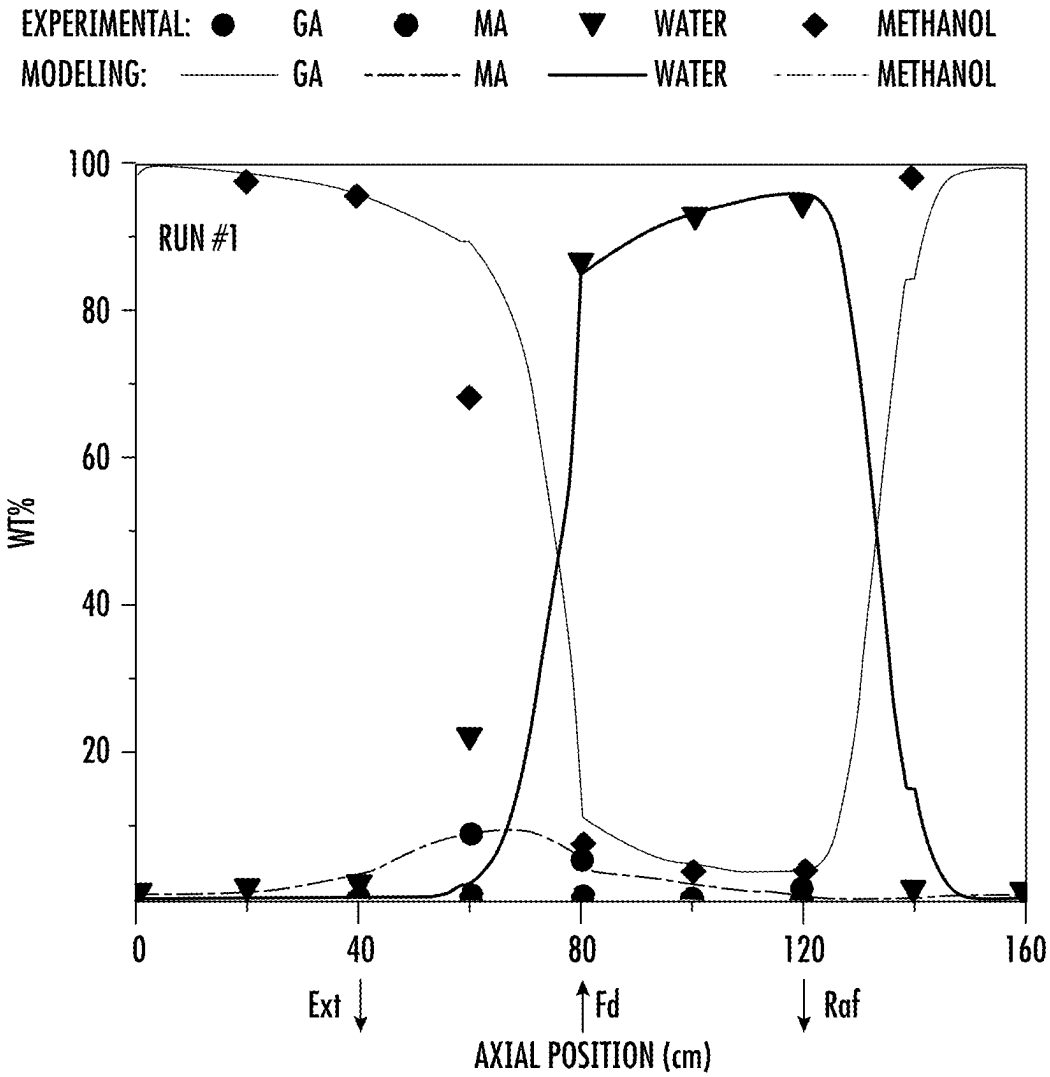
EXPERIMENTAL: GA MA WATER METHANOL
MODELING: GA MA WATER METHANOL
RUN #1
WT%
100
80
60
40
20
0
40
80
120
160
Ext
Fd
Raf
AXIAL POSITION (cm)

FIG. 9

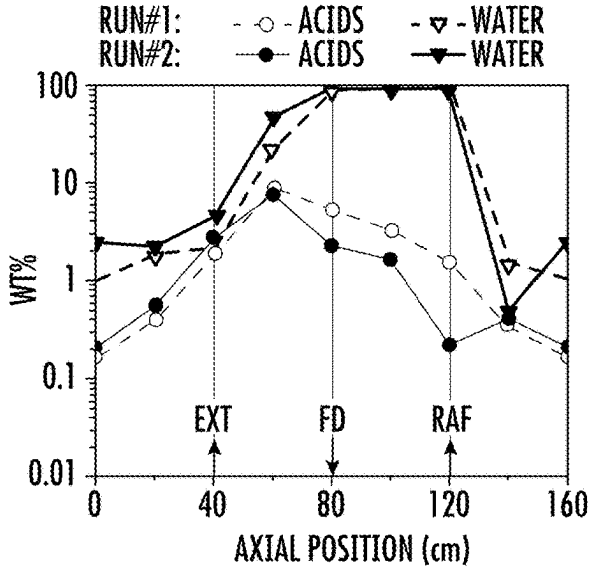

FIG. 10A

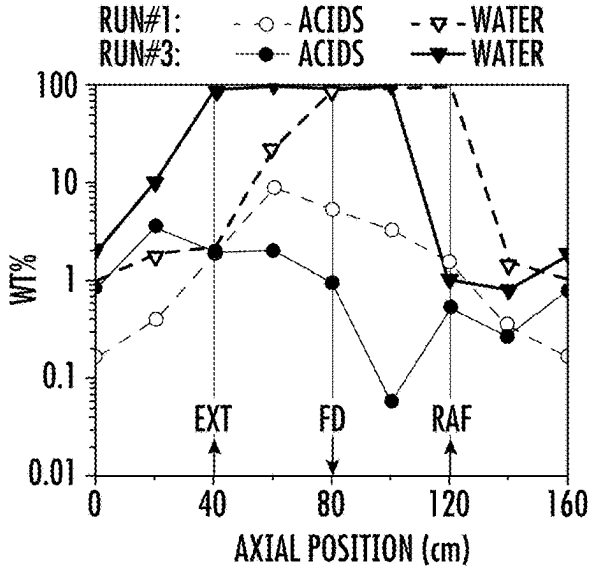

FIG. 10B

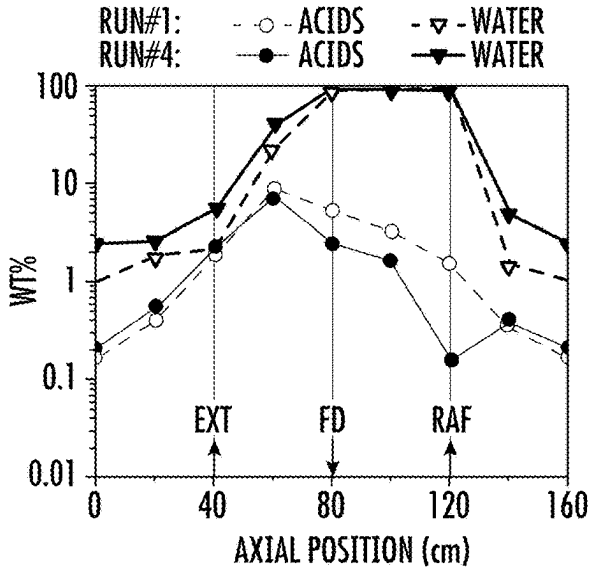

FIG. 10C

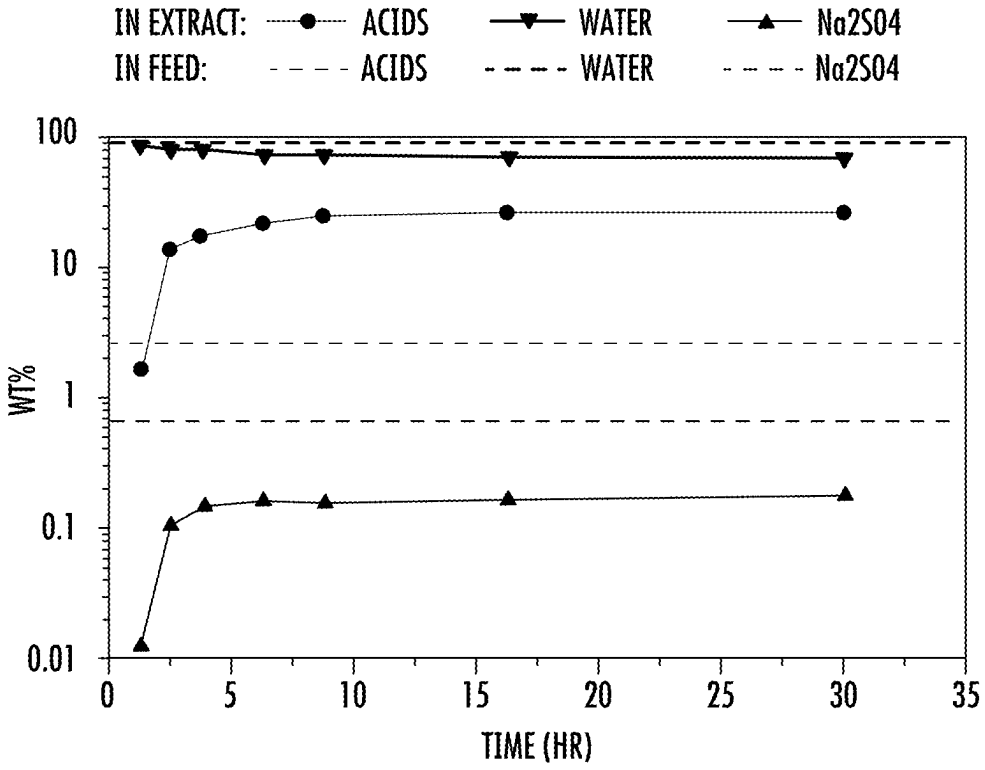

FIG. 11A

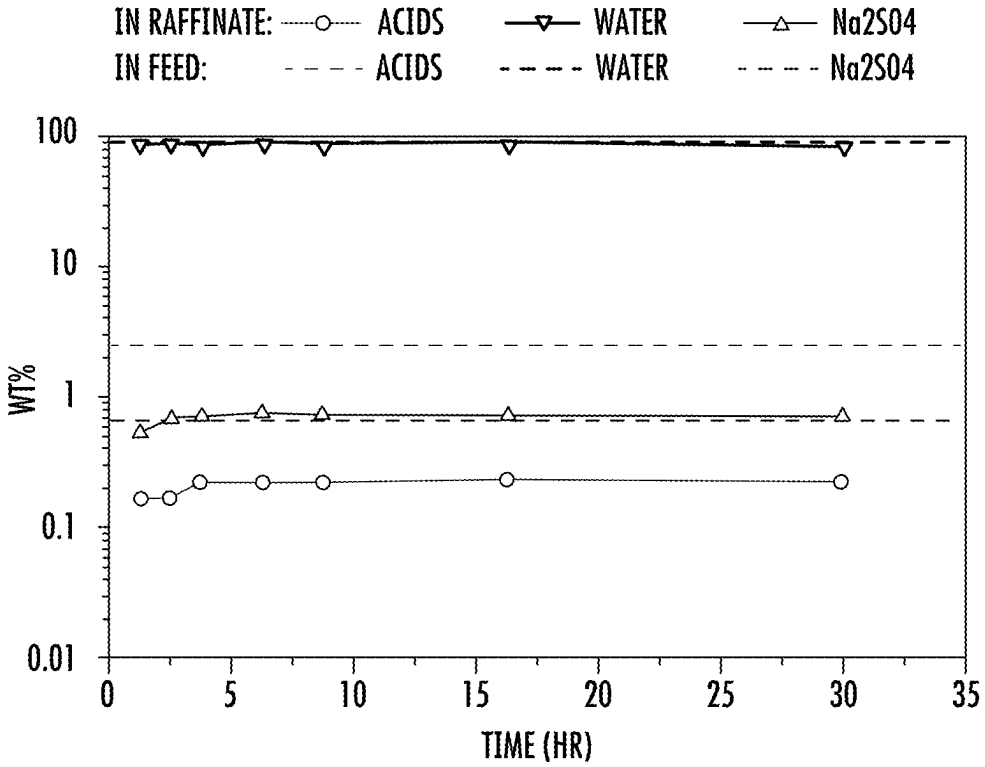

FIG. 11B

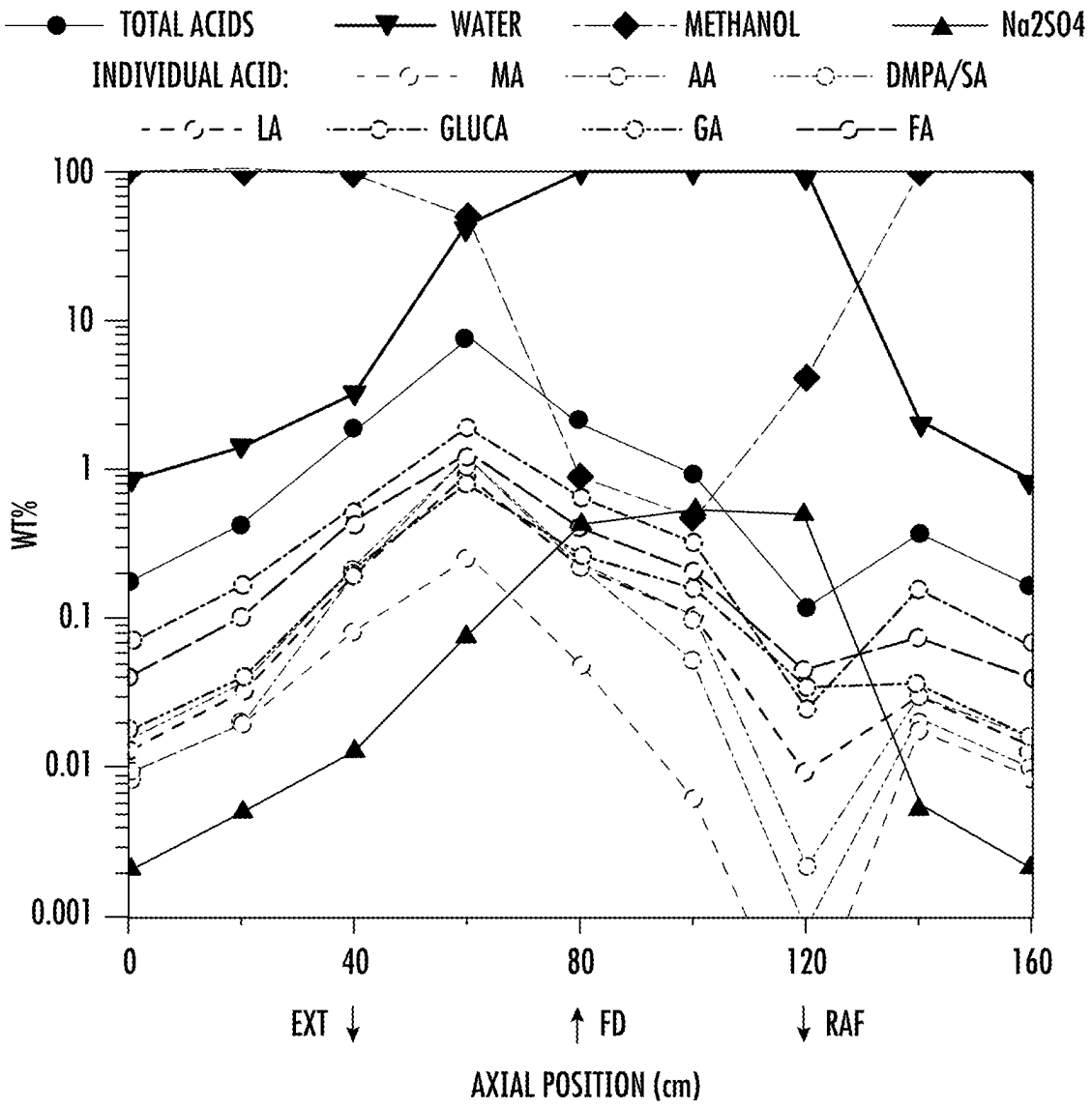
TOTAL ACIDS
WATER
METHANOL
Na2SO4
INDIVIDUAL ACID:
MA
AA
DMPA/SA
LA
GLUCA
GA
FA
100
10
1
0.1
0.01
0.001
WT%
0
40
80
120
160
EXT
FD
RAF
AXIAL POSITION (cm)

FIG. 12

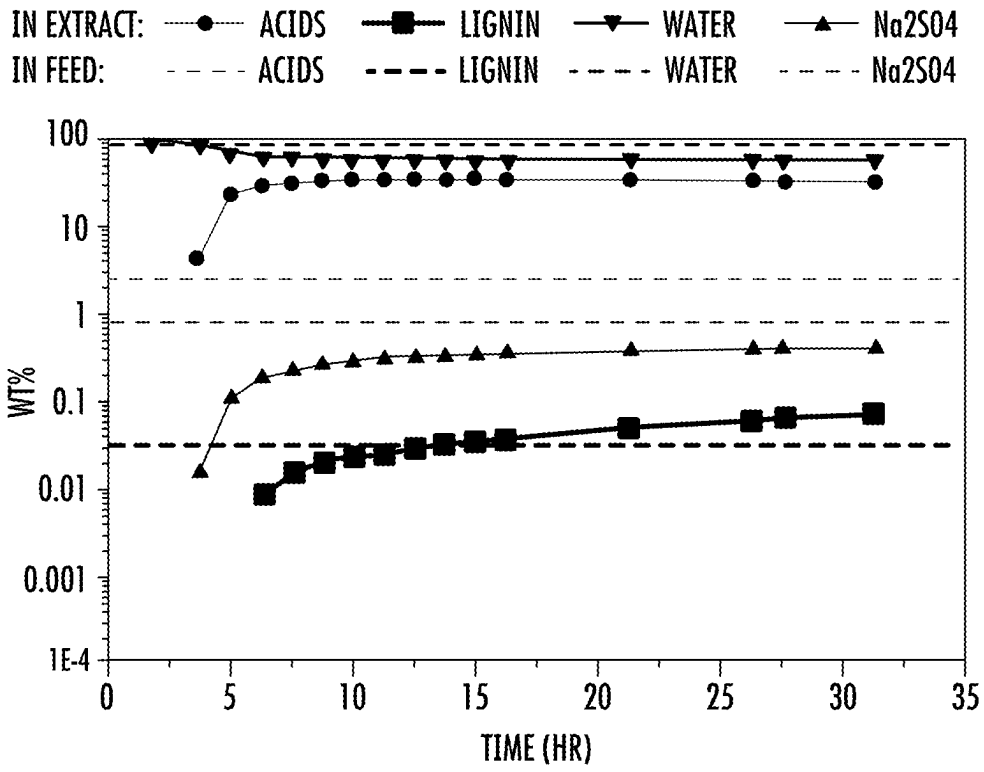

FIG. 13A

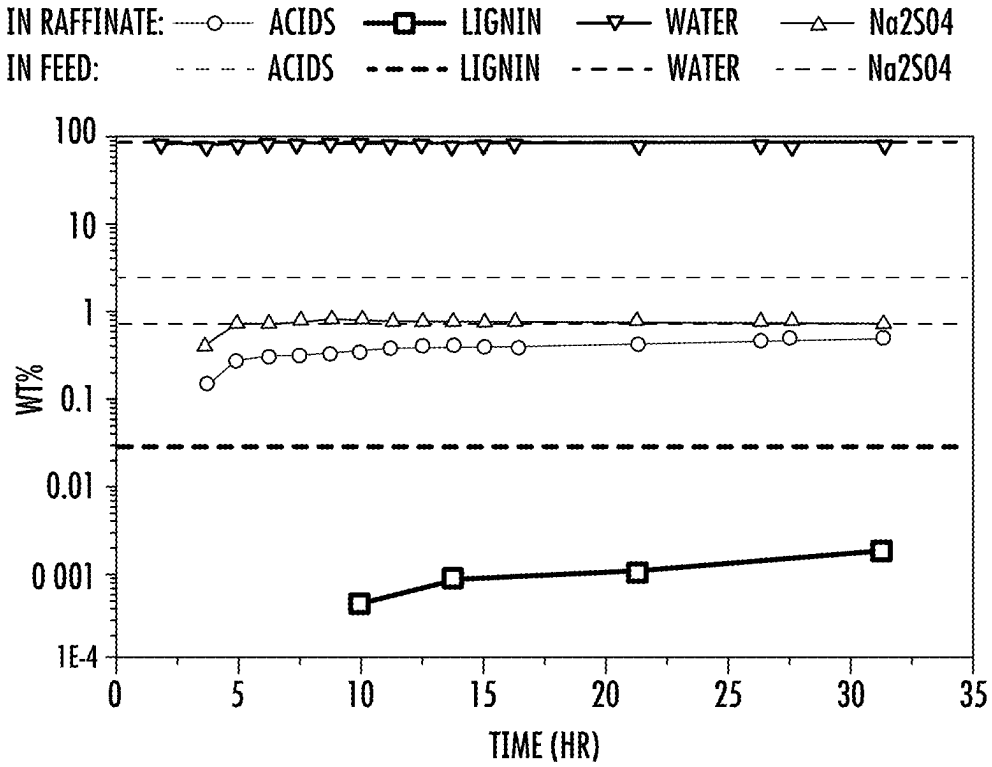

FIG. 13B

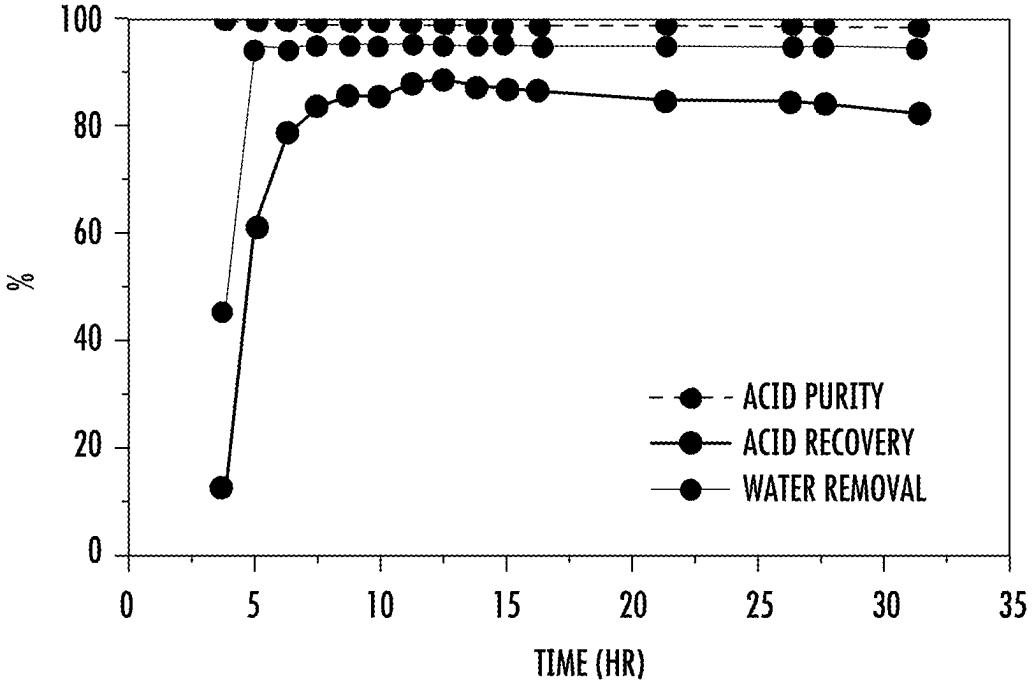
100
80
60
40
20
0
%
0
5
10
15
20
25
30
35
TIME (HR)
ACID PURITY
ACID RECOVERY
WATER REMOVAL

FIG. 14

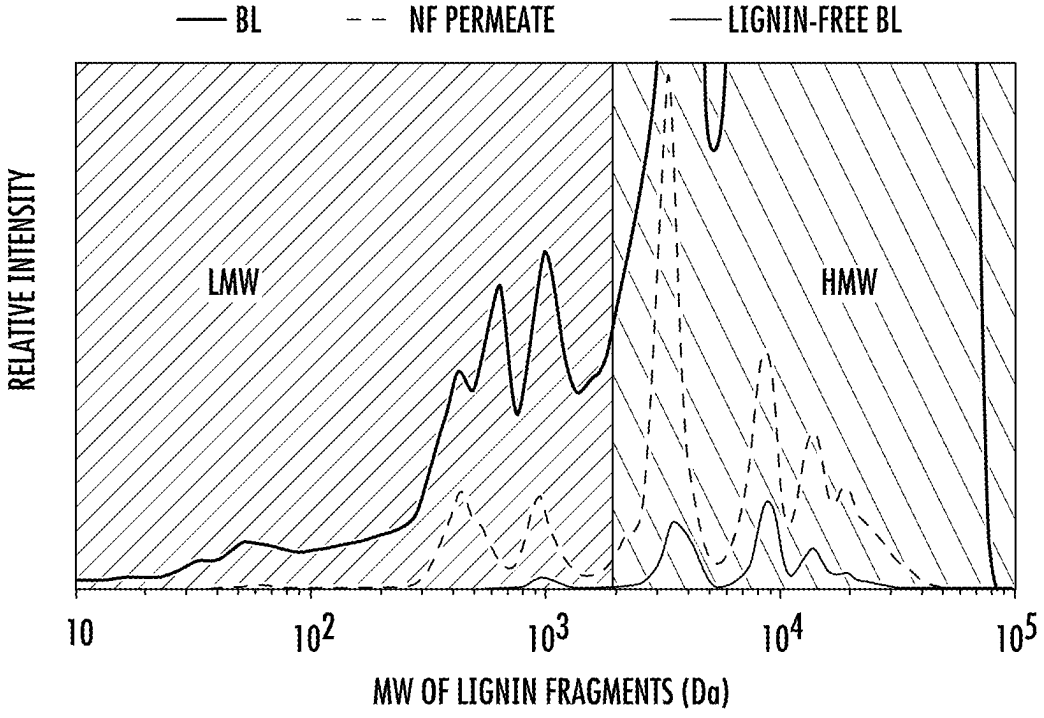
BL
NF PERMEATE
LIGNIN-FREE BL
RELATIVE INTENSITY
LMW
HMW
10
10^2
10^3
10^4
10^5
MW OF LIGNIN FRAGMENTS (Da)

FIG. 15

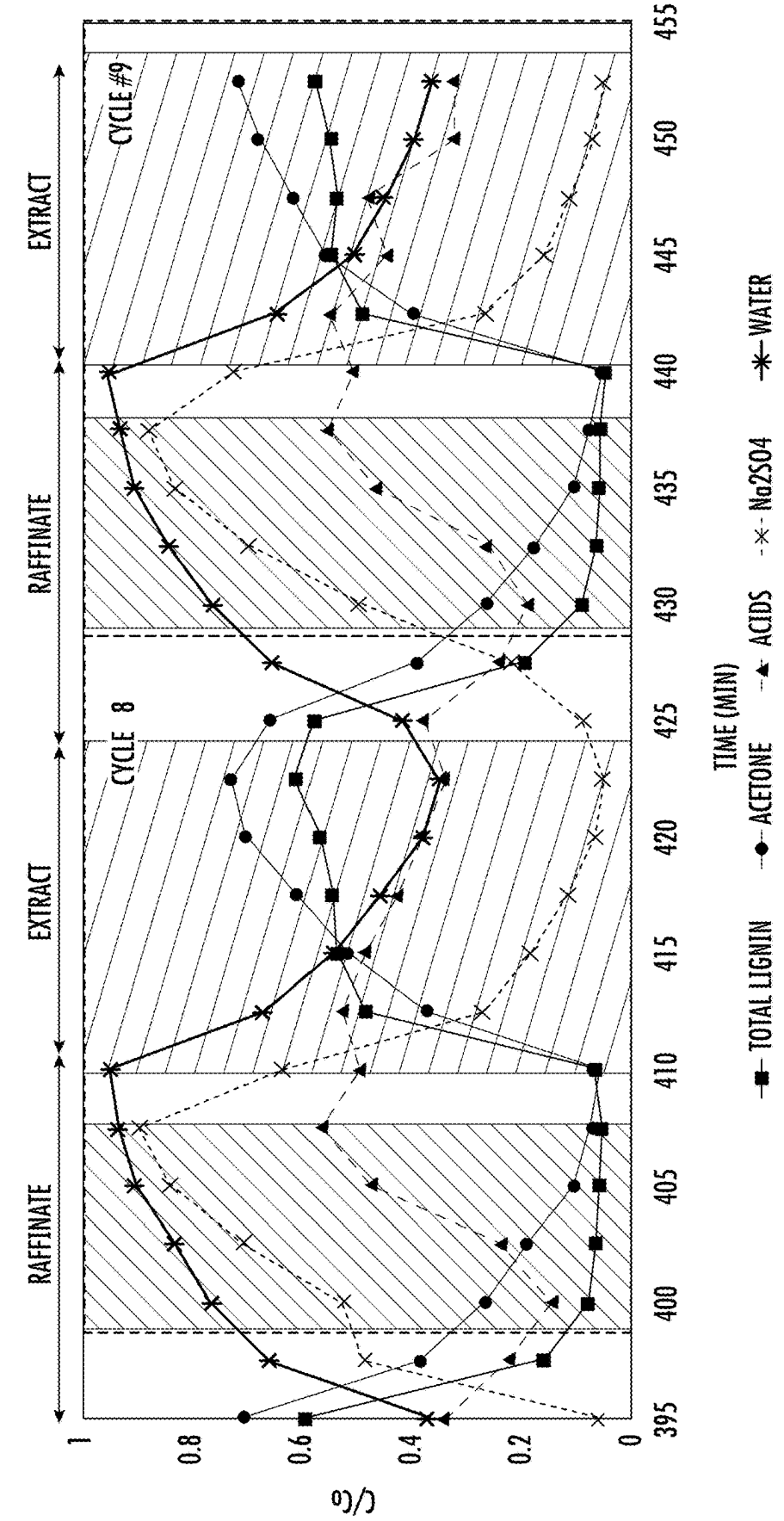
EXTRACT
RAFFINATE
EXTRACT
RAFFINATE
CYCLE #9
CYCLE 8
C/C0
1
0.8
0.6
0.4
0.2
0
395
400
405
410
415
420
425
430
435
440
445
450
455
TIME (MIN)
TOTAL LIGNIN
ACETONE
ACIDS
Na2SO4
WATER

FIG. 16

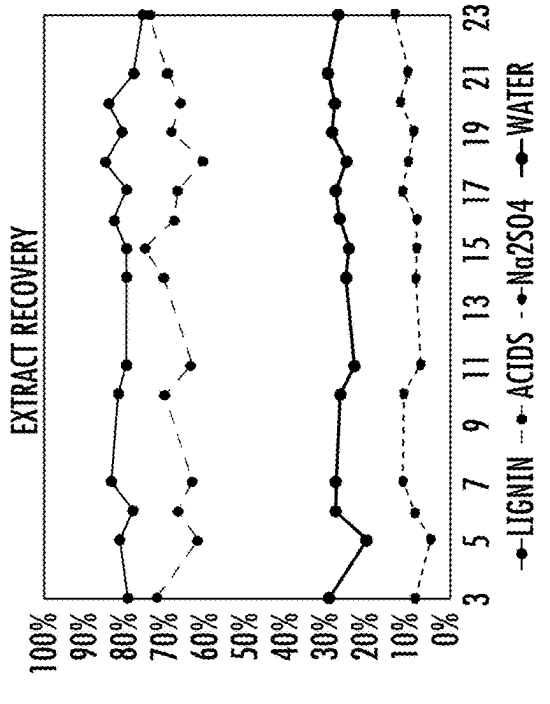

FIG. 17A

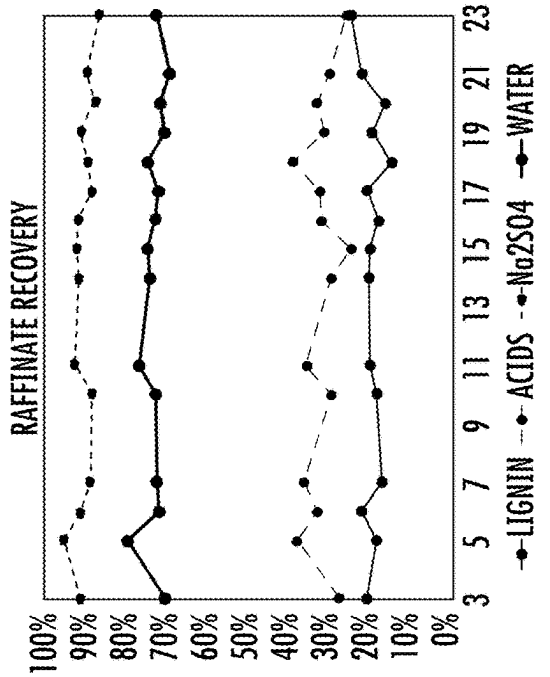

FIG. 17B

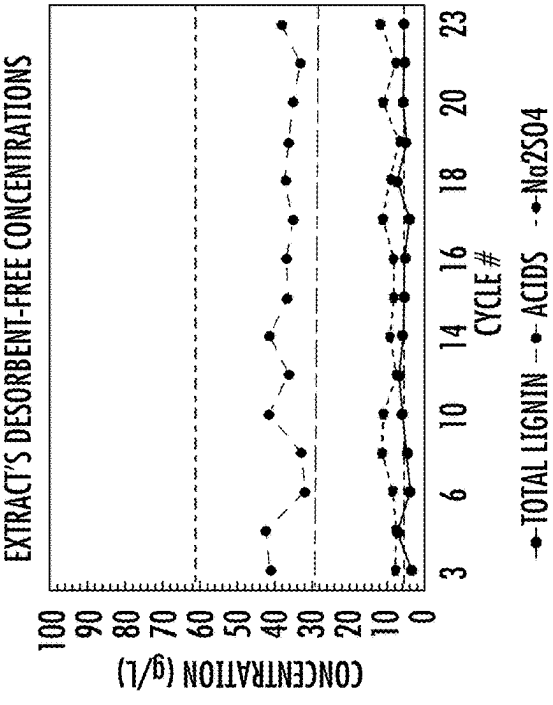

FIG. 17C

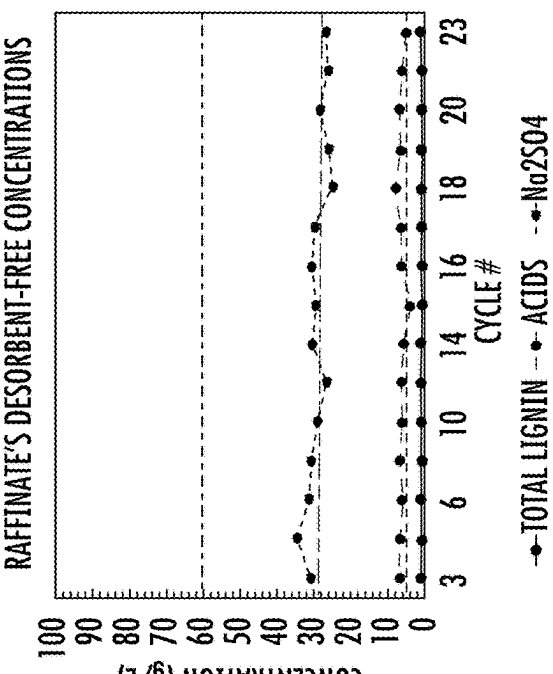

FIG. 17D

PROCESS FOR PRODUCTION OF LIGNIN, ORGANIC ACIDS, ORGANIC CHEMICALS, PURE CO2, AND WATER FROM KRAFT BLACK LIQUOR WITH OPERATIONAL EFFICIENCIES

CROSS-REFERENCE TO RELATED APPLICATIONS

[0001] This application claims the benefit of U.S. Provisional Application Ser. No. 63/553,482, filed on 14 Feb. 2024, which is incorporated herein by reference in its entirety as if fully set forth below.

FIELD OF THE DISCLOSURE

[0002] The present disclosure relates generally to systems and methods for processing black liquor feedstocks, and more particularly to integrated processes for production of lignin, organic acids, organic chemicals, pure CO_2, and water from kraft black liquor with operational efficiencies.

BACKGROUND

[0003] Kraft black liquor (BL) is a complex multicomponent byproduct of wood pulping. More than 6 tons of BL is generated for every ton of pulp produced. In a typical kraft process, BL is first dewatered by multiple-effect evaporators and then combusted in a recovery boiler to produce energy from the organic components and to recover the inorganic pulping chemicals as smelt. With the emergence of the sustainable integrated forest biorefinery concept, the valorization of BL-especially the biomass-derived organic components-is attracting increased attention.2 After lignin, the mixture of C1-C6 aliphatic carboxylic acids (including hydroxyacids) is the second main organic fraction in kraft BL. This mixture is the result of the decomposition of hemi-cellulose and cellulose during kraft pulping. More than 1.3 billion metric tons/yr of BL are generated in kraft processes worldwide, of which the organic acid fraction comprises at least 50 MMT/yr.3 Separation and purification of this fraction would provide a new, high-volume molecular feedstock for conversion into higher-value products such as fuels and lubricants.4-6 However, the development of viable separation processes is a significant challenge. A few works have proposed possible separation processes, but the high cost and lack of scalability of these processes are major barriers.

[0004] The production of chemicals and materials from renewable or circular resources is an important aspect of sustainable development. Utilization of biomass resources has been the subject of extensive research for sustainable production of commodity and specialty chemicals as well as liquid fuels. Lignocellulosic biomass (LCB) is the most abundant biomass resource, but it requires deconstruction (e.g., into various types of molecular feedstocks) before it can be upgraded by numerous proposed pathways. Because oxygen removal is a key step in the processing of biomass-derived feeds, many approaches involve supported metal catalysts under hydrogenating conditions. Over the years, researchers have designed and explored different catalytic systems to transform lignocellulose-derived carbohydrates including glucose to sorbitol, fructose to mannitol, furfural to furfuryl alcohol, furan, and tetrahydrofuran, among others Further upgrading of these intermediate products (sorbitol, mannitol, furfuryl alcohol, etc.) has been explored, targeting different platform chemicals, transportation fuels, and other products.

[0005] However, there remains a need in the art for improved processes for production of certain products from kraft black liquor with improved operational efficiencies, that address the high cost and lack of scalability of these processes. This disclosure provides a solution for this need.

BRIEF SUMMARY

[0006] An exemplary embodiment of the present disclosure provides a process for generating new products from a kraft mill and improving operational efficiency of a kraft mill through extraction of bioderived organic acids and liquid CO2 from weak black liquor generated during a kraft process, comprising the steps of: filtering a weak black liquor (BL) stream generated in the kraft process downstream from a brownstock washer to remove a first portion of lignin and generate a reduced lignin or de-lignified permeate and a retentate; removing the reduced lignin or de-lignified permeate from the kraft process; processing at least the de-lignified permeate to generate organic acids, liquid CO2, water, and raffinate containing salts; recovering the organic acids and liquid CO2; and returning the raffinate containing salts to the kraft process downstream of a recovery boiler.

[0007] In any of the embodiments disclosed herein, the process can comprise the step of, allowing the retentate of the filtered weak BL stream to remain within the kraft process.

[0008] In any of the embodiments disclosed herein, the process can comprise passing the reduced lignin or de-lignified permeate through a gas bubbler to generate an aqueous stream and a gas stream; passing the aqueous stream through an adsorption column to remove a second portion of lignin from the reduced lignin permeate to generate a delignified BL stream, and passing the delignified BL stream to a crystallizer to precipitate at least a portion of salt in the gas stream to generate a pretreated BL stream.

[0009] In any of the embodiments disclosed herein, the process can comprise passing the gas stream to a liquifying unit configured to liquefy the gas stream to liquid CO_2 and storing the liquid CO_2 and or using the liquid CO_2 for purposes other than the kraft process.

[0010] In any of the embodiments disclosed herein, the process can comprise the step of regenerating the adsorption column with an acetone-water mixture.

[0011] In any of the embodiments disclosed herein, the process can comprise processing step further comprises the steps of: removing, at least a portion of organic acids in the pretreated BL stream to generate a reduced-acid or acid-lean pretreated BL stream and converting the organic acids to one or more organic chemicals; and passing the reduced-acid pretreated BL stream through a reverse-osmosis membrane to generate the water and the raffinate containing salts.

[0012] An exemplary embodiment of the present disclosure provides a method of obtaining components from a kraft black liquor feedstock, comprising passing a BL feedstock through a NF membrane to remove a first portion of lignin in the BL feedstock to generate a NF permeate; acidifying, with an acidification unit, the NF permeate to generate an aqueous stream and an off-gas stream including CO_2; filtering, with a filtration unit, the aqueous stream to remove a second portion of lignin from the aqueous stream

to generate a delignified BL stream; removing, at least a portion of organic acids in the pretreated BL stream to generate a reduced-acid pretreated BL stream and a recovered organic acid stream; passing the reduced-acid pretreated BL stream through a membrane to generate a water permeate and a raffinate comprising salt and recovering the water permeate; passing the raffinate comprising salt through a membrane electrolyzer to generate an acidic stream and a basic stream; and liquifying gaseous CO_2 from within the off-gas stream into a liquified CO_2 stream and recovering the liquified CO_2 stream.

[0013] In any of the embodiments disclosed herein, the membrane electrolyzer can be or include a Bipolar Membrane Electrodialyzer (BMED).

[0014] In any of the embodiments disclosed herein, the method can further comprise causing one or more reactions between the at least a portion of the organic acids from the recovered organic acid stream and one or more catalysts to produce organic chemicals.

[0015] In any of the embodiments disclosed herein, the one or more reactions can comprise one or more reactions selected from the group consisting of deoxygenation, dehydroxylation, and oligomerization.

[0016] In any of the embodiments disclosed herein, the BL stream can comprise water, lignin, inorganic salts, and organic acids.

[0017] In any of the embodiments disclosed herein, the inorganic salts can comprise one or more salts selected from the group consisting of NaOH, Na_2S, $Na_2S_2O_3$, Na_2SO_4, Na_2HCO_3, Na_2CO_3.

[0018] In any of the embodiments disclosed herein, the NF membrane can be an alkali-stable NF membrane.

[0019] In any of the embodiments disclosed herein, the first portion of lignin in the BL feedstock can comprise at least 93% of lignin in the BL feedstock.

[0020] In any of the embodiments disclosed herein, the filtration unit includes a filter and the aqueous stream passing though the filter has a pH of at least 11.

[0021] In any of the embodiments disclosed herein, the second portion of lignin from the NF permeate can comprise at least 3% of lignin in the BL feedstock.

[0022] In any of the embodiments disclosed herein, passing the BL feedstock through a NF membrane further comprises, separating the NF permeate from a retentate, and wherein the BL feedstock is taken from a kraft process and the NF permeate is processed outside of the kraft process and wherein the retentate is returned to the kraft process.

[0023] In any of the embodiments disclosed herein, the acidifying step can include acidifying the NF permeate with H_2SO_4 to generate the aqueous stream and wherein the off-gas stream includes H_2S, SO_2, and CO_2.

[0024] In any of the embodiments disclosed herein, the method can include scrubbing the off-gas stream with a gas scrubber, wherein scrubbing includes introducing the off-gas stream and the basic stream into the gas scrubber and generating the gaseous CO_2 stream.

[0025] In any of the embodiments disclosed herein, passing the delignified BL stream through a gas bubbler can comprise introducing compressed air through a gas sparger.

[0026] In any of the embodiments disclosed herein, the aqueous stream from the gas bubbler can be acidified by H_2SO_4.

[0027] In any of the embodiments disclosed herein, the aqueous stream from the gas bubbler can be acidified by 98% H_2SO_4 to pH of about 2.5.

[0028] In any of the embodiments disclosed herein, passing the aqueous stream through a crystallizer, wherein the crystallizer can comprise MeOH.

[0029] In any of the embodiments disclosed herein, the MeOH can be maintained at about 60% v/v.

[0030] In any of the embodiments disclosed herein, bottom slurry of the crystallizer can be passed through a centrifuge and a filter press to produce Na_2SO_4 cake.

[0031] In any of the embodiments disclosed herein, the simulated-moving bed can utilize a methanol desorbent. In any of the embodiments disclosed herein, the simulated-moving bed can utilize an acetone desorbent.

[0032] In any of the embodiments disclosed herein, the removing step can include removing organic acids from the pretreated BL stream with a simulated-moving bed unit the simulated-moving bed can remove at least 90% of organic acids in the pretreated BL stream.

[0033] These and other aspects of the present disclosure are described in the Detailed Description below and the accompanying drawings. Other aspects and features of embodiments will become apparent to those of ordinary skill in the art upon reviewing the following description of specific, exemplary embodiments in concert with the drawings. While features of the present disclosure may be discussed relative to certain embodiments and figures, all embodiments of the present disclosure can include one or more of the features discussed herein. Further, while one or more embodiments may be discussed as having certain advantageous features, one or more of such features may also be used with the various embodiments discussed herein. In similar fashion, while exemplary embodiments may be discussed below as device, system, or method embodiments, it is to be understood that such exemplary embodiments can be implemented in various devices, systems, and methods of the present disclosure.

BRIEF DESCRIPTION OF THE DRAWINGS

[0034] FIG. **1***a* shows a schematic diagram of a conventional kraft process;

[0035] FIG. **1***b* shows a schematic diagram of an embodiment of a process in accordance with this disclosure, shown integrated into the conventional kraft process of FIG. **1***a;*

[0036] FIG. **1***c* shows a schematic diagram of an embodiment of a system in accordance with this disclosure, the system shown operating an exemplary embodiment of the process of FIG. **1***b;*

[0037] FIG. **2** depicts the expected reaction pathways during the HDO of an oxidation product of glucose;

[0038] FIGS. **3***a* and **3***b* show product distribution for the hydrodeoxygenation of model gluconic acid on 0.25% M/Nb2O5 (M=Pd, Pt, Rh, and Ru), where FIG. **3***a* shows without H2 coflow and FIG. **3***b* shows with H2 coflow;

[0039] FIGS. **4***a* and **4***b* show product distribution for the hydrodeoxygenation of model gluconic acid on 0.25% Pd/Nb2O5, where FIG. **4***a* shows product distribution at temperatures between 23° and 270° C. at 60 bar, 2.85 h-1, 50 mL/min H2 coflow and FIG. **4** shows product distribution at weight hourly space velocity (WHSV) between 1.43 and 4.28 h-1 (equivalent to 0.05 to 0.16 mL/min) at 60 bar, 250° C.;

[0040] FIGS. **5***a* and **5***b* show the catalytic performance of 0.25% Pd/Nb2O5 for the hydrodeoxygenation of model mixed hydroxy acids at temperatures between 24° and 280° C., where FIG. **5***a* depicts the conversion of individual hydroxy acids (gluconic acid (Gluc A), malic acid (MA), succinic acid (SA), glycolic acid (Glyc A), dimethylolpropionic acid DMPA, formic acid (Formic A), and Acetic Acid (Acetic A)), and FIG. **5***b* shows the product distribution;

[0041] FIGS. **6***a* and **6***b* shown catalytic performance of 0.25% Pd/Nb2O5 for the hydrodeoxygenation of kraft BL-derived hydroxy acids, where FIG. **6***a* shows total HA conversion and product distribution at temperatures between 265 and 295° C., and where FIG. **6***b* shows reactor configuration for the catalytic conversion of BL-derived HAs in accordance with this disclosure;

[0042] FIGS. **7***a* and **7***b* show catalytic performance of 0.25% Pd/Nb2O5 for the hydrodeoxygenation of kraft BL-derived hydroxy acids, where FIG. **7***a* shows the product distribution as a function of time-on-stream (TOS) at optimum reactor conditions (280° C., 60 bar, 1.0 h-1, 50 mL/min), and FIG. **7***b* shows the conversion and hydrodeoxygenation rate as a function of time-on-stream at optimum reactor conditions;

[0043] FIGS. **8***a* and **8***b* show a schematic representation of moving bed systems in accordance with this disclosure, where FIG. **8***a* depicts a true moving bed (TMB) system and FIG. **8***b* depicts a four-zone simulated moving bed (SMB) system with port switching and a 2-2-2-2 column configuration;

[0044] FIG. **9** shows a comparison of the experimentally measured internal concentration profiles (symbols) and model predictions (continuous curves) for an exemplary trial, Run #1, where the axial position scale represents the total length of the SMB columns (8 columns×20 cm/column=160 cm);

[0045] FIGS. **10***a*-**10***c* show the internal concentration profiles collected from exemplary trials, where FIG. **10***a* shows run #2, FIG. **10***b* shows run #3 and FIG. **10***c* shows run #4, which are indicated by a solid curve with closed dots;

[0046] FIGS. **11***a* and **11***b* show the composition of D-free extract and raffinate using a 9-component (8 synthetic acids+Na2SO4) feed stream over a 30-hour SMB run, where FIG. **11***a* depicts the extract and FIG. **11***b* depicts the raffinate;

[0047] FIG. **12** depicts the measured internal concentration profile from SMB steady-state operation with multi-component synthetic feed;

[0048] FIGS. **13***a* and **13***b* show the composition of D-free extract and raffinate using actual PBL as a feed stream over a 30 h SMB run, where FIG. **13***a* depicts the extract and FIG. **13***b* depicts the raffinate;

[0049] FIG. **14**, depicts SMB separation performance summary with the real PBL as the feed stream over a 30 h SMB run;

[0050] FIG. **15** shows a comparison between the molecular weight distributions (MWDs) of lignin in the kraft BL, partially delignified BL (NF permeate), and highly delignified ("lignin-free") PBL;

[0051] FIG. **16** shows normalized concentration profiles of outlet streams from exemplary trials, cycle #8 and #9, of cyclic fixed-bed adsorption;

[0052] FIGS. **17***a*-**17***d* show recovery of lignin, acids, Na2SO4, and water to extract and raffinate; and desorbent-free concentration profiles of extract and raffinate streams over 23 cycles, where FIG. **17***a* shows recovery of lignin, acids, Na2SO4, and water to extract, FIG. **17***b* shows recovery of lignin, acids, Na2SO4, and water to raffinate, FIG. **17***c* shows desorbent-free concentration profiles of extract, and FIG. **17***d* shows desorbent-free concentration profiles of raffinate.

DETAILED DESCRIPTION

[0053] To facilitate an understanding of the principles and features of the present disclosure, various illustrative embodiments are explained below. The components, steps, and materials described hereinafter as making up various elements of the embodiments disclosed herein are intended to be illustrative and not restrictive. Many suitable components, steps, and materials that would perform the same or similar functions as the components, steps, and materials described herein are intended to be embraced within the scope of the disclosure. Such other components, steps, and materials not described herein can include, but are not limited to, similar components or steps that are developed after development of the embodiments disclosed herein.

[0054] Various embodiments of the present disclosure describe processes, which can be integrated with current kraft pulping processes to produce concentrated lignin, concentrated organic acids, chemicals from conversion of the organic acids, pure CO_2, and reusable water from weak black liquor. The processes disclosed herein can allow for the production of value-added products from the kraft process as well as facile capture of significant quantities of CO_2 for storage/sequestration. Furthermore, one of the important operational efficiencies can result from the reduction of inorganic salt content entering the multi-effect evaporators, thereby reducing scaling of evaporators.

[0055] In accordance with at least one aspect of this disclosure, FIGS. **1***b* and **1***c*, show a process **100** which can be integrated with current kraft pulping processes (e.g., as shown in FIG. **1***a*) to produce concentrated lignin, concentrated organic acids, chemicals from conversion of the organic acids, pure CO2, and reusable water from weak black liquor. Embodiments of the process **100** allows for the production of value-added products from the kraft process as well as facile capture of significant quantities of CO2 for storage/sequestration. Furthermore, embodiments can provide operational efficiencies resulting from the reduction of inorganic salt content entering the multi-effect evaporators, thereby reducing scaling of evaporators.

[0056] An exemplary process for obtaining components from a kraft black liquor feedstock is shown highlighted in FIG. **1***b* and shown in isolation in FIG. **1***c*. Various embodiments of the present disclosure can include one or more of the steps shown in FIGS. **1***b* and **1***c*. Though certain percentages at various steps are shown in FIGS. **1***b* and **1***c* and discussed below, the present disclosure is not so limited. The exemplary process **100** shown in FIGS. **1***b* and **1***c* includes, providing a black liquor (BL) feedstock **150** to a processing system **200**. The feed stream **150** for the process **100** shown in FIGS. **1***b* and **1***c* can comprise water, lignin, inorganic salts, and organic acids. In certain embodiments, the BL stream **150** can be a weak black liquor from Kraft process (e.g., as shown in FIG. **1***b*), which typically comprises about 15 wt % total solid comprising water, lignin, inorganic salts (NaOH, Na_2S, Na_2S_{203}, Na_2SO_4, Na_2HCO_3, Na_2CO_3), and organic acids. Further description of embodiments of the weak BL feedstock is included in the discussion of experimental example 1 described later.

[0057] The process **100** comprises, at step S**101**, passing the weak BL feedstock **150** through a nanofiltration (NF) membrane to remove a first portion of lignin in the BL feedstock **150** to generate a retentate **152** and retain a second portion of lignin in the BL feedstock **150**, generating NF permeate **154**. As shown in FIG. **1***b*, the retentate **152** can be kept within the kraft process, while the NF permeate **154** is passed through process **100** for further processing. In certain embodiments, the first portion of lignin (e.g., the portion removed from the BL feedstock **150** and retained in the retentate **152** can comprise at least 93% of lignin. The second portion of lignin from (e.g., the portion retained by the NF permeate **154**) can comprise at least 3% of lignin.

[0058] At step S**102**, the process **100** includes separating the NF permeate **154** into an aqueous stream **156** and a gas stream **158**. In certain embodiments, the process can further include acidifying the aqueous stream **156**, for example by introducing H_2SO_4. In certain embodiments, acidifying the aqueous stream can include acidifying by 98% H_2SO_4 to pH of about 2.5 In certain embodiments, the process **100** can additionally include, at step S**107**, scrubbing the gas stream and at step S**108**, liquifying the gas stream **160** to generate liquid CO_2.

[0059] At step S**103**, the process **100** includes passing the aqueous stream **156** through a filter to remove the second portion of lignin from the aqueous stream, removing lignin particles precipitated during the acidification step to generate an aqueous delignified BL stream **160**. The precipitated lignin is removed from the stream **160** and collected.

[0060] In certain embodiments, the step S**104** can further include removing, with a simulated-moving bed (SMB) unit, at least a portion of organic acids in the pretreated BL stream to generate a raffinate (referred to as reduced-acid pretreated BL stream **162**) and organic acids extract **164**. In certain embodiments, the SMB unit can utilize a methanol or acetone desorbent and can be configured and adapted to remove at least 90% of organic acids in the pretreated BL stream. In certain embodiments, the process **100** can additionally include, further processing of the extract **164**, for example, by causing one or more reactions (e.g., catalytic conversion) between the at least a portion of organic acids and one or more catalysts to produce organic chemicals. The one or more reactions can include deoxygenation, dehydroxylation, and oligomerization, to produce the organic chemicals.

[0061] The process **100** further includes, at step S**105**, passing the reduced-acid pretreated BL stream **166** through a reverse-osmosis membrane to generate a raffinate **166** comprising salt and a water permeate **167**. The water permeate **167** can be collected and used for other purposes within a Kraft mill but outside Kraft process, for example for power generation.

[0062] At step S**106**, the raffinate **166** comprising salt can be passed to a membrane electrolyzer to generate an acidic stream **168** and a basic stream **170**. In step S**107**, the basic stream **170** can be passed to a gas scrubber, which is used to scrub the off gas stream **158** generated in step S**102**, producing an alkaline stream and a CO_2 gas stream. At Step S**108**, the CO_2 gas stream is liquified to liquid CO_2 and sequestered or used for other purposes outside of Kraft process. In certain embodiments, the membrane electrolyzer can be or include a Bipolar Membrane Electrodialyzer (BMED).

[0063] Still with reference to FIG. **1**, the system **200** will be described. The system **200** includes a first unit **201**. The weak BL feedstock **150** is fed into the first unit **201** which includes a nanofiltration (NF) membrane therein configured to remove a first portion of the lignin from the weak BL feedstock **150**. The NF membrane can be or include an alkali-stable nanofiltration membrane, configured to retain over 93% lignin from the weak BL feedstock **150**, and allow a large fraction of inorganic salts, organic acids, and water from the weak BL feedstock **150** to pass through the membrane. From the unit **201**, the BL feedstock **150** is divided into retentate **152** and NF permeate **154**. The retentate **152** from the membrane can be a lignin product and some of these products can be removed for lignin utilization. The retentate **152** is returned to the kraft process, e.g. at the evaporators shown in FIG. **1***b*, while the NF permeate **154** continues through the process **100**, outside of the kraft process. The retentate **152** can have much lower concentration of salts than in a conventional kraft process, thereby reducing scaling of the evaporators and thereby improving operational efficiencies.

[0064] The system **200** includes unit **202**, which receives the NF permeate **154**. The product from unit **202** includes an aqueous stream **156** and a gas stream **158**. The aqueous stream **156** can be acidified in the acidification tank by 98% H_2SO_4, lowering the pH of the aqueous stream **156** to a pH of about 2.5. In certain embodiments, acidification of the aqueous stream **156** can occur in a cooled acidification tank, which can be cooled to about 25 C. The gas stream **158** generated in this acidification tank (such as H_2S and SO_2, and CO_2 can be passed to a unit **207** (downstream caustic scrubber), and a unit **208** to generate liquid CO_2, which will be described further later.

[0065] In the unit **203**, the aqueous stream **156** can be passed through a filter unit. In certain embodiments, the aqueous stream **156** passing through the filter unit can have a pH >11), where 3% residual lignin can be captured by the filter, to produce a raffinate, referred to as delignified BL stream **160**. The concentration of lignin in the delignified BL stream **160** from this column can be maintained below 1 g/L before column regeneration.

[0066] The system **200** includes unit **204**, configured to recover organic acids from the filtrated delignified BL stream **160** into extract stream **164**. The unit **204** separates the delignified BL stream **160** into the extract stream **164** and the raffinate stream **162**. The raffinate stream **162** will be salt-rich. This stream **162** is concentrated further in a membrane in unit **205** to produce a low salt permeate, which can be used recycled water, and a high-salt stream **166**. This high salt stream **166** is fed into the membrane electrolyzer unit to produce base (stream **170**) and acid (stream **168**). The base stream is used as scrubbing solution for off gas stream **158** in the gas scrubber unit **207**. The purified stream of CO_2 from gas scrubber is liquified in liquefaction unit **208**. Part of the acid stream can be returned to the acidifier unit **204** or purged to keep the Na/S balance. In certain embodiments, to avoid the organic-solvent-induced salt precipitation, instead of the traditional sequence of alternating feed and desorbent into the adsorption bed as used with cyclic fix-bed adsorption, two "wash" streams of low-salt water are introduced between adsorption/desorption steps to dilute sulfur salts and acetone. This operational design prevents salt precipitation inside the adsorption column, thereby avoiding high pressure drops and blockage of activated carbon pores.

[0067] In certain embodiments, the unit **204** can also include, a simulated-moving bed (SMB) unit configured to receive the pretreated BL stream. Further description of embodiments of the SMB can be found in the description of experimental example 2 described later. The SMB can continuously recover organic acids from the pretreated stream, generating the raffinate (reduced acid pretreated BL stream **162**) and the extract **164** containing organic acids. Before, SMB, the pretreated BL stream **160** can comprise around 3 wt % organic acids, 0.01 wt % lignin, 0.05 wt % inorganic acids salt, and water. In certain embodiments, the desorbent can be pure methanol due to low boiling point and heat of evaporation. In certain embodiments, the desorbent can be acetone. Acetone is advantageous as a solvent because it can desorb both lignin and organic acids, has a higher solubility for sulfate salts compared to methanol, and is thermodynamically easier to recover from water, with a larger vapor-liquid equilibrium (VLE) gap even at 1 atm. Additionally, acetone's heat of evaporation (518 KJ/kg) is roughly half that of methanol (1180 KJ/kg), reducing energy requirements for recovery. Accordingly, in certain embodiments, the SMB can recover above 90% organic acids from the pretreated feed **160** into extract stream **164** with 95% water removal rate. In certain embodiments, the methanol in the extract **164** and raffinate (reduced acid pretreated BL stream **162**) can then be recovered by a distillation column. In certain embodiments, the extract **164** can be further processed in a conversion unit, which will be discussed further below.

[0068] The system **200** further includes unit **205**, which can be or can include a reverse-osmosis membrane or a nanofiltration membrane configured to receive the reduced acid pretreated BL stream **162**. The reverse osmosis membrane can produce high-purity water stream (water permeate) **167** from solvent-free reduced acid pretreated BL stream **162** under pressure (e.g., 66 bar in certain embodiments). This recovered high-purity water permeate **167** can be used in later processing, for example for bleaching or pulp washing units, while the raffinate stream **166** with high salt concentration can be used in late stages of brownstock washing units. The system **200** includes unit **206**, which can comprise a membrane electolyzer, configured to receive the salty raffinate **166** from the unit **205**, to generate an acidic solution **168** and a basic solution **170**. The basic solution **170** can be fed to the downstream caustic scrubber, unit **207**.

[0069] The system **200** can also include unit **208**, configured to liquify theCO_2 generated from unit **202** during the acidification process, as discussed above, and from the scrubber **207**. The unit **208** can be configured to liquify the captured CO_2 by the Linde-Hampson process. For example, in certain embodiments, the gas stream **158** from the acidification unit (e.g., unit **202**) can be first compressed to (e.g., to 19.7 bar) and cooled (e.g., to 35 C) with a heat exchanger before flashed to remove water in a flash tank. The dehumidified CO_2 stream can be further compressed (e.g., to 100 bar) and cooled (e.g., to 24 C) with a series of heat exchangers before flashing the stream at a pressure (e.g., 19.7 bar) adiabatically to produce liquified CO_2 with less than 100 ppm H_2O, which can be sequestered or released as treated effluent into the mill's stack.

[0070] The system **200** can further include one or more additional units, configured and adapted for catalytic conversion of the organic acids generated in the unit **204**, e.g., for processing the extract stream **164**. For example, in certain embodiments, the organic acids in extract stream **164** can be converted by a mixture of catalysts to produce organic chemicals by reactions such as deoxygenation, dehydroxylation, and oligomerization. The resulting mixtures can be used as valuable specialty products that substitute petroleum-derived products in several applications (e.g., lubricants, waxes, additives).

[0071] In accordance with another embodiment of the process, the process comprises, passing the BL feedstock through a nanofiltration (NF) membrane to remove a first portion of lignin in the BL feedstock to generate a retentate and retain a second portion of lignin in the BL feedstock, generating NF permeate. The retentate can be kept within the kraft process, while the NF permeate is passed through the embodiment of the novel process for further processing. In certain embodiments, the first portion of lignin (e.g., the portion removed from the BL feedstock and retained in the retentate can comprise at least 93% of lignin. The second portion of lignin from (e.g., the portion retained by the NF permeate) can comprise at least 3% of lignin.

[0072] The process can include passing the NF permeate through a granular activated carbon (GAC) absorption column to remove the second portion of lignin from the NF permeate to generate a delignified BL stream. In certain embodiments, the process can additionally include, regenerating the adsorption column with acetone-water mixture, for example, using acetone present at 50% v/v water, and in certain embodiments, the acetone-water mixture can be at 50° C.

[0073] The concentration of lignin in the delignified BL stream from this column can be maintained below 1 g/L before column regeneration. In certain embodiments, the adsorption column can be regenerated with injection of acetone, for example, the adsorption column in unit **202** can be regenerated with 50% v/v acetone water at 50° C. for regeneration. After, in certain embodiments, 100% acetone can be recovered from distillate of a distillation column while the bottom stream can contain mainly water and residual lignin be recycled for pulp washing unit. Acetone is advantageous as a solvent because it can desorb both lignin and organic acids, has a higher solubility for sulfate salts compared to methanol, and is thermodynamically easier to recover from water, with a larger vapor-liquid equilibrium (VLE) gap even at 1 atm. Additionally, acetone's heat of evaporation (518 KJ/kg) is roughly half that of methanol (1180 KJ/kg), reducing energy requirements for recovery.

[0074] The process can include passing the delignified BL stream through a gas bubbler to generate an aqueous stream and a gas stream. Passing the delignified BL stream through a gas bubbler can comprise introducing compressed air through a gas sparger. In the gas bubbling unit, compressed air (2-3 bar, in certain embodiments) is introduced through the gas sparger. In certain embodiments, the bubbling unit can be kept at 70° C., and the air bubble retention time can range from 10 to 15 min. The product includes an aqueous stream and a gas stream **160**. The aqueous stream coming from the gas bubbling unit can be acidified in the acidification tank by 98% H_2SO_4, lowering the pH of the aqueous stream to a pH of about 2.5. In certain embodiments, acidification of the aqueous stream can occur in a cooled acidification tank, which can be cooled to about 25 C. In certain embodiments, the process can further include acidifying the aqueous stream from the gas bubbler, for example by introducing H_2SO_4. In certain embodiments, acidifying

the aqueous stream can include acidifying by 98% H_2SO_4 to pH of about 2.5 In certain embodiments, the process can additionally include liquifying the gas stream to generate liquid CO_2. In certain embodiments, gases generated during acidification, such as H_2S and SO_2, can be captured by a downstream caustic scrubber.

[0075] The process can further include passing the aqueous stream to a crystallizer to precipitate at least a portion of salt in the aqueous stream, to generate a pretreated BL stream and a salt cake. In certain embodiments, crystallizing can include crystallizing the stream using MeOH, for example, MeOH maintained at about 60% v/v. In certain embodiments, the process can additionally include passing a bottom slurry of the crystallizer through a centrifuge and a filter press to produce the Na_2SO_4 salt cake. The acidified aqueous stream can be pumped into the crystallizer in which MeOH is kept at 60% v/v for the precipitation of Na_2SO_4 salt. A bottom slurry from the crystallizer can be passed through a centrifuge and a filter press to produce Na_2SO_4 cake. A majority of this Na_2SO_4 can be returned to a recovery boiler for balance of process Na/S, for example, in certain embodiments, the acidic stream, containing 0.65 M H_2SO_4 and 0.05 M Na_2SO_4, can be recycled back to the acidifier with part of this stream purged for potential use in crude tall oil (CTO) production. The effluent from CTO production can then be returned to multi-effect evaporators. A supernatant with inorganic salt concentration can be below 8 g/L. Still within the crystallizer of unit **204**, the acidified aqueous stream can be pre-heated by the bottom product of the MeOH distillation column to generate pretreated BL stream. The MeOH distillation column can be configured and adapted to recover above 99.0% MeOH with 95% distillate solvent purity. The bottom product can contain mainly water, inorganic salt, and organic acids which can be further cooled down by the incoming supernatant stream and cooling water to 25 C.

[0076] In certain embodiments, to avoid the organic-solvent-induced salt precipitation, instead of the traditional sequence of alternating feed and desorbent into the adsorption bed as used with cyclic fix-bed adsorption, two "wash" streams of low-salt water are introduced between adsorption/desorption steps to dilute sulfur salts and acetone. This operational design prevents salt precipitation inside the adsorption column, thereby avoiding high pressure drops and blockage of activated carbon pores.

[0077] Further, the process can comprise, removing, with a simulated-moving bed (SMB) unit, at least a portion of organic acids in the pretreated BL stream to generate a reduced-acid pretreated BL stream and organic acids extract. In certain embodiments, the SMB unit can utilize a methanol or acetone desorbent and can be configured and adapted to remove at least 90% of organic acids in the pretreated BL stream. In certain embodiments, the process can additionally include, further processing of the extract, for example, by causing one or more reactions (e.g., catalytic conversion) between the at least a portion of organic acids and one or more catalysts to produce organic chemicals. The one or more reactions can include deoxygenation, dehydroxylation, and oligomerization, to produce the organic chemicals.

[0078] The SMB can continuously recover organic acids from the pretreated stream, generating a reduced acid pretreated BL stream. The GAC's high surface area and the selective adsorption of organic acids over water and salts allow for high acids recovery and water removal from the pretreated black liquor stream by the unit. The pretreated BL stream can comprise around 3 wt % organic acids, 0.01 wt % lignin, 0.05 wt % inorganic acids salt, and water. In certain embodiments, the desorbent can be pure methanol due to low boiling point and heat of evaporation. Accordingly, in certain embodiments, the SMB can recover above 90% organic acids from the pretreated feed into extract stream with 95% water removal rate. In certain embodiments, the methanol in the extract and raffinate (reduced acid pretreated BL stream) can then be recovered by a distillation column. In certain embodiments, the extract can be further processed in a separate unit.

[0079] For example, this separate unit can be configured and adapted for catalytic conversion of the organic acids generated acidification tank. For example, in certain embodiments, the organic acids in extract stream **167** can be converted by a mixture of catalysts to produce organic chemicals by reactions such as deoxygenation, dehydroxylation, and oligomerization. The resulting mixtures can be used as valuable specialty products that substitute petroleum-derived products in several applications (e.g., lubricants, waxes, additives).

[0080] The process further includes, passing the reduced-acid pretreated BL stream through a reverse-osmosis or nano filtrate membrane to generate a water permeate and a raffinate comprising salt. The reverse osmosis or nanofiltrate membrane can produce high-purity water stream (water permeate) from solvent-free reduced acid pretreated BL stream under pressure (e.g., 66 bar in certain embodiments). This recovered high-purity water permeate can be used in later processing, for example for bleaching or pulp washing units, while the raffinate stream with high salt concentration can be used in late stages of brownstock washing units.

Examples and Experimental Analysis

[0081] The following description relates to example embodiments and accompanying experimental analysis, and the disclosed technology is not limited to these example embodiments.

Experimental Example 1—Catalytic Upgrading of a Mixed Hydroxy Acid Feedstock Derived from Kraft Black Liquor

[0082] Lignocellulosic feedstocks are widely studied for sustainable liquid fuel and chemical production. The pulp and paper industry generates large amounts of kraft black liquor (BL) from which a high volume of hydroxy acids (HAs) can be separated for further catalytic processing. Disclosed herein is an examination of catalytic upgrading of HAs, including the conversion of (1) a model HA, gluconic acid; (2) a model mixture of HAs, and (3) a real mixture of HAs derived from kraft BL on M/Nb2O5 (M=Pd, Pt, Rh, and Ru). The hydrodeoxygenation of model gluconic acid reveals that "volatile" carboxylic acids (mainly C2 and C3), levulinic acid, and cyclic esters are significant products over all the catalysts, with Pd/Nb2O5 showing superior activity and selectivity toward valuable intermediates. The model mixture of Has shows a wide range of reactivity over the supported metal catalyst, with the product selectivity strongly correlating to reaction temperature. Utilizing a 0.25% Pd/Nb2O5 catalyst, a real mixture of HAs derived from kraft BL is successfully dehydroxylated to produce a mixture rich in C3-C8 carboxylic acids that may be ame-

nable for further upgrading, e.g., catalytically to ketones with high carbon chain lengths. Despite the feedstock complexity, we selectively cleaved the C—OH bonds of HAs, while successfully preserving most of the —COOH groups and minimizing C—C and C—O bond scission reactions under the operating conditions tested. The BL-derived HA stream is thus proposed to be a suitable platform for producing mixed carboxylic acid products from an overoxygenated byproduct feed.

[0083] Many intermediate products can be formed during the hydrodeoxygenation (HDO) of the biomass-derived carbohydrates substrates resulting from the hydrogenolysis of C—C, C—O, —O—C—O, and C═O bonds. For instance, FIG. **2** depicts the expected reaction pathways during the HDO of an oxidation product of glucose (i.e., gluconic acid). In FIG. **2**, route (a) produces hydroxy acids with lower carbon atoms (such as lactic, glycolic, and malic acids), typically owing to incomplete C—OH removal. Meanwhile, in route (b), reaction conditions favor the complete cleavage of the C—OH bonds to form carboxylic acids of varying carbon numbers. Route (c) is the direct hydrogenation of the C═O carbonyl group of HAs to alcohols whereas (d) represents C—C cleavage on metal sites forming aldehydes with the release of CO2 and/or CO via decarboxylation and decarbonylation, respectively. Route (e) is the ketonic decarboxylation of carboxylic acids to ketones, (f) is the ring opening reaction of γ-valerolactone (a cyclic ester) to form pentanoic acid on strong acid sites, and (g/h) represent a combination of hydrogenation, dehydration, and cyclization reactions, due to intramolecular interactions between hydroxyl and carbonyl groups. The complexity of these pathways, with different bond cleavages occurring, suggests the importance of developing a catalytic system capable of selectively cleaving a specific type of bond from the biomass-derived oxygenates toward achieving a target product.

[0084] Transition metals (especially, Pd, Rh, Pt, and Ru) have been conventionally employed in the HDO of biomass oxygenates owing to their ability to activate hydrogen into a form that is suited for the C—O removal process. In many research studies, the roles of metal sites have been extensively studied using model and real carbohydrate feedstocks. For instance, during the HDO of sorbitol, Pd and Pt metal sites played the role of hydrogenating C—O and C~O bonds formed during the dehydration reaction. The metal sites additionally catalyzed the C—C bond cleavage reaction leading to decarboxylation/decarbonylation products. In another investigation that assessed the roles of metals (Ru, Pt) in glycerol hydrogenolysis, it was noted that the more a metal possesses available unoccupied orbitals, the more likely it is to drive C—C bond cleavage reactions. Despite the crucial roles of metal sites in HDO reactions, they sometimes do not offer satisfactory activity and selectivity to target products. Hence, noble metals are typically combined with acidic solid supports to form bifunctional metal-acid site pairs.

[0085] With the presence of metal-support interactions, the metal site can enable the spillover of activated hydrogen atoms to the surface of the support, thereby facilitating the hydrogenation of chemical bonds. Thus, the metals perform the role of dissociating H2 and delivering the dissociated H atoms to the oxygenate, while the support provides the catalytic site for the surface reaction of the oxygenate and the H atoms. Consequently, the efficiency of the metal is improved. Toward elucidating the role of support sites, several candidates including activated carbon, e.g., ZrO2, TiO2, Nb2O5, etc. have been explored. In selecting the support materials, properties such as hydrothermal stability, the potential to sinter metal particles, the strength and density of acid sites, and other factors are important. Sintering of metal particles can depend on the nature of the metal oxide support. For instance, a study reported very quick and heterogeneous sintering of Pt particles on SiO2 and Al2O3supports; however, these particles are stable on ZrO2. In another investigation, strongly acidic TiO2-WOx supported on various metals (Ir, Pd, Pt) showed very good hydrothermal stability.

[0086] The removal of the —OH functional groups in biomass oxygenates via C—O hydrogenolysis can be achieved either directly on metal sites or over bifunctional sites via stepwise dehydration and hydrogenation reactions. Meanwhile, in different systems involving the catalytic transformation of oxygenates, monometallic catalysts on carbon supports (e.g., Pt/C, Pd/C, etc.) have been observed to preferentially drive C—C cleavage reactions rather than C—O bond cleavage. Since the dehydration reaction step is catalyzed by the strong acid sites of the support, studies have explored the roles of many support materials. An example is the study of C—C and C—O hydrogenolysis in glycerol over Pd and Ru supported on ZrO2 and ZrO2/WO3. The electron density of the metals is reduced on ZrO2 compared to the ZrO2/WO3 dual support. The addition of WO3 on the ZrO2 support enhanced the electron density of the metals, thereby inhibiting the C—C cleavage reaction. This was attributed to the increase in the density of acid sites in the dual support relative to ZrO2 alone, thereby favoring the C—O bond cleavage reaction. Another study using Pt supported on Nb2O5 and Vulcan carbon also found the strong acidity of Nb2O5 in the upgrading of lactic acid to favor C—O bond cleavage, relative to C—C bond cleavage.

[0087] Furthermore, depending on the oxygenate feed and target products, bimetallic catalysts can be superior to monometallic catalysts. The catalytic bifunctionality can be achieved either via metal/metal or metal/metal-oxide interactions. The addition of a second metal modifies the activity of the first metal by shifting its d-band density of states. For example, Dumesic et al. designed an approach to convert carbohydrates to hydrocarbons using a combination of different catalytic systems (for example as discussed in "Integrated Catalytic Conversion of γ-Valerolactone to Liquid Alkenes for Transportation Fuels," Science (1979) 2010, 327 (5969), 1110-1114, the entirety of which is herein incorporated by reference). A flow reactor packed with a Pt—Re/C catalyst drove the conversion of polyols and sorbitol to liquid organic products consisting of alcohols, ketones, carboxylic acids, and heterocyclic compounds. Ideally, C—C bond cleavage is more favored on Pt for oxygenated feedstocks than C—O bond cleavage. Meanwhile, a second metal (i.e., Re with oxophilic properties) modified the selectivity toward favoring C—O cleavage. However, most of the proposed mechanisms for HDO involves dual sites, with the oxide support providing the site for C—O activation. This can be achieved by metal/metal-oxide interaction, especially when the metal oxide has oxophilic properties (e.g., Fe2O3, Nb2O5, etc.).

[0088] Black liquor (BL) is generated in large amounts (estimated >1 billion metric tons/year globally) in the pulp and paper industry utilizing the kraft process. In addition to lignin, inorganic sulfur salts, alkali, and carbonates, BL

contains a range of C1-C6 acids. A typical kraft mill generating 4 MMT/yr of BL can produce about 0.1-0.2 MMT/yr of hydroxy acids (HAs). BL-derived HAs have 1-2 carboxylic (—COOH) groups and 0-5 hydroxy (—OH) groups. The total concentration of HAs in kraft BL is 3-5 wt %, comparable to the concentration of lignin and inorganics in BL. The carboxylic acids in BL contain volatile acids (formic acid and acetic acid) and nonvolatile compounds as well (hydroxy mono/dicarboxylic acids and dicarboxylic acid). In the context of this example study, the entire carboxylic acid mixture is collectively referred to as "hydroxy acids" (HAs). During the delignification of wood in the kraft pulping process, the carbohydrates (i.e., mainly cellulose and hemicellulose) undergo a primary peeling reaction in alkaline pH at high temperatures (>80° C.) to form different aliphatic carboxylic acids, with the elimination of the monosaccharide units. The peeling reaction competes directly with a stopping reaction that avoids the complete degradation of carbohydrates into carboxylic acids that are not conducive to an alkaline peeling reaction.

[0089] Ideally, a greater extent of peeling of hemicellulose is expected relative to cellulose owing to its lower degree of polymerization as well as its amorphous structure. Since the content of cellulose and hemicellulose varies in different wood types, optimization of the kraft pulping operating conditions to modulate the composition of the hydroxy acids would be beneficial for catalytic conversion purposes. In current practice, the HAs are instead combusted along with lignin in the recovery boiler, thereby generating steam and electricity. Since the heating value of the carboxylic acid fraction is ~50% less relative to lignin in BL,44 a significant effect of isolating the carboxylic acids on the energy supply of the paper mill is not expected. Thus, the recovery and subsequent valorization of the carboxylic acid stream to produce products with high market value is worthwhile. Recently, separation processes based on graphene oxide membranes and granulated activated carbon adsorbents have been developed for the scalable and continuous fractionation of BL into lignin-rich and HA-rich streams. In particular, HA streams with >90% acid purity are produced. This advance enables the use of the HA stream as a feedstock for producing value-added chemicals via a heterogeneous catalysis pathway.

[0090] One of the challenges for catalytic conversion is the complexity of the overoxygenated HA feedstock, exhibiting species with different structures, functionalities (C—O, —COOH, —OH), and overall composition. As shown in the expected reaction pathways in FIG. **2**, the production of carboxylic acids via route (b) is preferred, as its further upgrading via ketonization reactions to increase the carbon chain length is well-established in the literature. This requires the development of an appropriate catalytic dehydroxylation system to remove the —OH functional groups via selective C—O bond cleavage while preserving other functional groups (i.e., C—O and COOH), and minimizing C—C bond cleavage reactions. To achieve this, a bifunctional catalyst comprising a metal site in synergy with a strong acid site is preferred. This is because the presence of strongly acidic support can improve the hydrogenation efficiency of metals, and the strong metal-oxygen bond formed from this synergy is required to drive the HDO of biomass oxygenates. Group VIIIB transition metals (e.g., Pt, Pd, Ru, and Rh) are known for their excellent ability, they favor C—C bond cleavage relative to C—O bond cleavage when supported on carbon. However, when used in tandem with reducible supports (Nb2O5, TiO2, CeO2, and ZrO_2), C—C bond cleavage can be suppressed.

[0091] The strong metal-support interaction created when metals are supported on reducible metal-oxides has been shown to correlate with excellent HDO activity relative to nonreducible supports like Al2O3, SiO_2, etc. Particularly, Nb2O5 is an interesting support for our application owing to its hydrothermal stability, redox properties, its ability to promote C—O bond cleavage reactions, its oxophilicity, and its suitable acidity. In an investigation where a noble metal was supported on Al2O3, TiO2, ZrO2, and Nb2O5, the niobia provided the lowest C—O bond-breaking energy for phenol, suggesting its ability to strongly adsorb the C—O bond and reduce its dissociation energy, consequently promoting C—O bond cleavage. More so, the Nb4+/Nb5+ of Nb2O5 can act as an oxophilic site that can strongly adsorb the oxygen in the oxygenate substrate, thereby contributing to excellent adsorption of oxygenates on Nb2O5 and promoting the activation of C—O bonds. Hence, the presence of a strong acid support like Nb2O5 in the catalytic system is a viable strategy to efficiently supply H atoms for the target reaction.

[0092] Some of the acids making up the HAs (such as lactic acid and succinic acid) have been individually studied for catalytic conversion. For instance, lactic acid can react over Pt/Nb2O5 to form mainly acetaldehyde and propionic acid. To the best of our knowledge, no previous works have attempted to catalytically upgrade a complex mixture of model or realistic C1-C6 hydroxy acids sourced from the kraft pulping process. Accordingly, embodiments of a process shown and described herein includes the first known demonstration of the catalytic upgrading of model and realistic kraft black liquor-derived hydroxy acids on bifunctional catalysts. An overall objective for the catalytic upgrading of kraft BL-derived HAs involves the conversion of the enriched C1-C6 HA feedstock to C15-C40 range (partially or fully) deoxygenated mixtures. Here, the focus is primarily on the first upgrading step, i.e., bifunctional catalysis to remove the —OH functionality via C—OH bond scission reactions. Catalytic experiments were systematically performed under different reaction conditions and feeds, and the results were analyzed in the context of understanding the substrate reactivity. First, gluconic acid (2,3,4,5,6-pentahydroxyhexanoic acid), a C6 monocarboxylic acid with 5-OH groups, was used as a model substrate to understand the reactivity of highly oxygenated HAs. Then, a complex model mixture of eight HAs with varying carbon number and OH content was studied. Finally, the conversion of a real HA mixture separated from a kraft BL, containing 27 different acids was studied. Overall, the HA feed is converted to a mixture of carboxylic acids, ketones, aromatics, esters, and hydrocarbons (removing up to 60% of the oxygen), along with some CO2 generation. Thus, embodiments of the novel process shown and described herein demonstrate that real HA feedstocks can serve as a platform to produce intermediates suitable for further catalytic upgrading into higher-value products, such as lubricants, waxes, and other materials.

[0093] Due to the complexity of the HA mixture derived from the kraft process, initial catalytic experiments were conducted using model acids. The aliphatic carboxylic acids isolated from kraft BL are mainly composed of volatile acids (formic acid and acetic acid), hydroxy acids with 2-4 carbon

atoms (mainly glycolic acid, lactic acid, 2-hydroxybutanoic acid, and 2,5-dihydroxypentanoic acid), and isosaccharinic acids with 5-6 carbon atoms (mainly gluco- and xylo-isosaccharinic acids). Some of these predominant carboxylic acids in kraft BL have been upgraded. For example, the utilization of the volatile components of the carboxylic acids (formic and acetic) via pathways like ketonization and catalytic transfer hydrogenation is well established in the literature (see, for example, Pham et al., "Ketonization of Carboxylic Acids: Mechanisms, Catalysts, and Implications for Biomass Conversion" ACS Catal. 2013, 3 (11), 2456-2473; and Gilkey, Xu, "Heterogeneous Catalytic Transfer Hydrogenation as an Effective Pathway in Biomass Upgrading" ACS Catal. 2016, 6 (3), 1420-1436, both of which are incorporated by reference herein in their entirety). More so, studies on 2-hydroxypropanoic acid (i.e., lactic acid) via different catalytic systems to produce valuable platform chemicals have been reported. Particularly, the work of Dumesic and coworkers on lactic acid C—O hydrogenolysis to propanoic acid is insightful for understanding the behavior of similar hydroxy acids with higher carbon atoms, for example as discussed in Serrano-Ruiz et al. "Catalytic Processing of Lactic Acid over Pt/Nb2O5" ChemSuschem 2009, 2 (6), 581-586, the entire content of which is incorporated by reference herein. Hence, studying the reactivity of isosaccharinic acids via HDO pathways is crucial to have a complete understanding of the hydroxy acid mixture derived from kraft BL. Here, gluconic acid (a product of glucose oxidation) was selected as a model HA for individual study. This choice is justified because it is commercially available and possesses similar structural properties with the α- and β-saccharinic acid (i.e., gluco- and xylo-isosaccharinic acids) components of the BL which contribute ~28 wt % of the realistic hydroxy acid mixture.

[0094] Gluconic acid possesses multiple oxygenated functional groups, low volatility, high water solubility, high reactivity, and low vapor pressure. Its conversion was in the aqueous phase at suitable high pressure and mild temperatures. Qualitative and quantitative analyses of reaction products were achieved using gas chromatography-mass spectrometry (GC/MS) and a combination of gas chromatography and high-performance liquid chromatography (GC/HPLC), respectively Initially several group VIIIB metals were screened as catalysts for the C—OH bond cleavage of the model gluconic acid molecule, specifically Pd, Ru, Rh, and Pt-supported on Nb2O5, due to their known hydrogenolysis activity and strong acidity, respectively. Pt/C was reported to be an efficient catalyst for C—C bond scission relative to C—O bond scission. However, the presence of acidic sites provided by Nb2O5 (i.e., Pt/Nb2O5 catalyst) favored the C—O bond cleavage via a 2-step reaction (dehydration-hydrogenation). Thus, the HDO of gluconic acid was tested with different nominal loadings of Pd (0.1-1.0 wt %) on the Nb2O5 support. The activity for gluconic acid HDO increased with increasing metal loading. At the lowest metal loading of 0.1 wt % Pd, about 25% of the converted carbon constitutes undesired hydroxy acids, which significantly decreased to ~3% at 1 wt % Pd loading. The selectivity to desired target species such as carboxylic acids, levulinic acid, and esters is similar and more favorable at Pd loadings ≥0.25 wt %. Distinctively, an increasing selectivity to xylitol (a C5 sugar alcohol) was observed with increasing Pd loading (from ~2% at 0.1 to ~11% at 1.0 wt % loading), formed via C~O cleavage of the carbonyl group. Hence, in all the screening experiments, 0.25 wt % nominal metal (Pd, Ru, Rh, or Pt) loading was deemed sufficient to drive the hydrodeoxygenation (HDO) of gluconic acid.

[0095] In preliminary experiments utilizing >20 wt % gluconic acid concentration, reactor clogging leading to poor quantification of the product stream was observed, as well as difficulty in dislodging the postreaction content of the reactor. Thus, a concentration of ~11 wt % was selected to study the reactivity of gluconic acid during HDO reaction. The catalysts were operated at low reactant conversions (i.e., <10%, differential reactor conditions) at 2.85 h-1 weight hourly space velocity (WHSV) of gluconic acid. All four catalysts showed similar conversions of 6-8% and selectivities to the desired products such as carboxylic acids, esters, and ketones. The initial results suggested that all the catalysts can potentially drive HA conversion under these conditions, with the Pd and Pt catalysts indicating slightly higher activity and a more desirable product distribution with lower COx evolution.

[0096] Carbohydrate feedstocks such as glucose and polyols can typically undergo simultaneous deoxygenation and reforming reactions over bifunctional catalysts. During reforming, the carbohydrate-derived feedstock can adsorb on the metal sites and dehydrogenate via C—C cleavage to form H2 and CO2 via the water-gas shift reaction. The in situ-generated H2 can then drive the hydrogenolysis and hydrogenation reactions. Hence, gluconic acid conversions were conducted at a higher temperature (230° C., 60 bar, and 2.85 h-1), with and without H2 coflow.

[0097] FIGS. **3***a* and **3***b* show product distribution for the hydrodeoxygenation of model gluconic acid on 0.25% M/Nb2O5 (M=Pd, Pt, Rh, and Ru) (FIG. **3***a*) without H2 coflow and (FIG. **3***b*) with H2 coflow. Operating conditions: 230° C., 60 bar, 0.1 mL/min (equivalent to 2.85 h-1), 50 mL/min H2 coflow. Steady-state data were taken after 5 h on-stream, HAs represent organic acids containing-OH functional groups, HCs represent hydrocarbons, and wherein carbon recovery: 86-89%. These Figs. depict the product selectivity. Overall, the gluconic acid conversion is significantly higher with H2 coflow (79-94%) than without (50-68%). This suggests that in the case of in situ H2 generation, the amount of formic acid generated is insufficient to provide the H2 required to drive the conversion of gluconic acid comparable to that obtained with H2 coflow. Additionally, FIGS. **3***a* and **3***b* shows large differences in product selectivity between the two cases. Without H2 coflow, undesirable products containing-OH functionalities (arabi-nose, lactic acid, glutaric acid, glycolic acid, etc.) are formed significantly. The remaining (desirable) products are distributed between volatile carboxylic acids, ketones, esters, alcohols, aldehydes, and hydrocarbons.

[0098] In contrast, H2 coflow shows a large increase in the selectivity to desirable products. The Pd-based catalyst showed the highest selectivity to C1-C6 carboxylic acids and esters, while the selectivity to levulinic acid is similar on both Pt and Pd catalysts. Among the ester products, up to 87% was contributed by γ-valerolactone (GVL), gluconic acid y-lactone, and gluconic acid 8-lactone over the 0.25% Pd/Nb2O5 catalyst, which was the highest selectivity to cyclic esters among the current four catalysts. The data suggest that 0.25% Pd/Nb2O5 can efficiently cleave the C—OH bonds of gluconic acid to produce mainly levulinic acid (a keto acid), carboxylic acids, and cyclic ketones. The levulinic acid undergoes dehydration and hydrogenation on

metal-acid sites to form GVL,70 while the gluconic acid lactones were formed via the cyclization of gluconic acid. 19 Further the niobia-supported metal catalysts were compared with carbon-supported metals at the same conditions (i.e., low conversion). All catalysts supported on carbon revealed lower activity relative to metal/niobia catalysts. However, there was observed a noticeable increase in selectivity to acids (including levulinic acid) and a decrease in the selectivity to esters, probably due to the absence of acid sites to drive dehydration reactions.

[0099] Moreover, the M/carbon catalysts cleaved the C~O bond of gluconic acid to form C5 and C6 sugar alcohols (sorbitol and xylitol). All metal/carbon catalysts show some generation of CO2 (no CO was identified), which became more significant with an increased reaction temperature. Gluconic acid can adsorb on the metal-acid sites and undergo decarboxylation and decarbonylation (C—C bond scission), dehydrogenation (C—H bond scission), or hydrogenation and dehydration (C—O bond scission) to form reactive intermediates (see, e.g., FIG. **2**). The selectivity toward CO2 and alkane/alkene hydrocarbons is highest over Rh and Ru catalysts, indicating that they increased the rate of C—C bond cleavage relative to C—O bond scission. Overall, the 0.25% Pd/Nb2O5 catalyst offered the most desirable conversion, carbon balance, and highest selectivity to intermediate oxygenates (e.g., esters, ketones, and C1-C6 carboxylic acids) that are good intermediates for the synthesis of value-added products.

[0100] Characterization techniques, including H2 chemisorption, ammonia temperature-programmed desorption (TPD), and N2 physisorption, were used to probe the physiochemical properties of the supported metal catalysts. Table 1, shown below, displays the physiochemical properties of the supported metal catalysts used in this study, including the total acid sites, metal dispersion, active particle diameter, and N2 physisorption parameters for all of the catalysts, where [a]S/A=BET surface area, PV=pore volume, PR=pore radius, [b]N2 physisorption, [c]H2 Chemisorption, [d]ammonia temperature programmed desorption.

TABLE 1[a]

Catalysts	S/A[(b)] (m^2/g)	PV[(b)] (cm^3/g)	PR[(b)] (nm)	Active d_p[(c)] (nm)	Dispersion[(c)] (%)	Acid sites[(d)] (μmol/g)
0.25Pd/Nb_2O_5	144	0.30	4.9	1.9	58	641
0.25Pt/Nb_2O_5	132	0.25	5.0	4.3	31	632
0.25Rh/Nb_2O_5	135	0.26	4.9	2.7	39	623
0.25Ru/Nb_2O_5	137	0.25	5.1	14.1	10	512
Nb_2O_5	163	0.31	4.9	—	—	896
0.25Pd/Nb_2O_5 (used)	94	0.19	5.2	—	—	—

[0101] The supported metal catalysts exhibited lower total acidic sites (512-641 μmol/g) relative to the bare acidic niobia support (896 μmol/g) due to partial coverage of the Nb2O5 surface with the metal domains. The significant variation in the total acid sites in the supported metal (with the highest being 641 μmol/g for 0.25% Pd/Nb2O5) suggests that the metal domains exhibited different coordination with the surface of Nb2O5.71 All catalysts exhibit typical Type III isotherms with hysteresis in the adsorption-desorption curves, resulting in a mesopore distribution. Among the supported metal catalysts, 0.25% Pd/Nb2O5 revealed the highest BET surface area (141 m2/g) and pore volume (0.30 cm3/g). H2 pulse chemisorption was employed to elucidate the metal dispersion and the average particle diameter. As seen in Table 1, the metal dispersion follows the order Pd>Rh>Pt>Ru, with the 0.25% Pd/Nb2O5 showing ~58% overall dispersion. This indicates that the Pd-based catalyst afforded the surface of acidic Nb2O5 with the highest fraction of exposed Pd metal atoms for C—OH bond scission. The catalytic performance exhibited by 0.25% Pd/Nb2O5 can thus be attributed to relatively more uniform Pd dispersion, high specific surface area, and high total acid sites, as confirmed by the characterization results. Hence, we selected a 0.25% Pd/Nb2O5 catalyst for subsequent experiments.

[0102] Next, a wider range of operating conditions (temperature, WHSV, and pressure) was explored to guide the subsequent processing of the more complex mixed HA feedstock. Gluconic acid is thermally unstable, and it is important to convert it at a sufficiently low temperature to minimize the contribution of degradation reactions. Generally, gluconic acid conversion increased with temperature, achieving close to 100% conversion at 250° C. FIGS. **4***a* and **4***b* show product distribution for the hydrodeoxygenation of model gluconic acid on 0.25% Pd/Nb2O5 at (FIG. **4***a*) temperatures between 23° and 270° C. at 60 bar, 2.85 h-1, 50 mL/min H2 coflow and (FIG. **4***b*) weight hourly space velocity (WHSV) between 1.43 and 4.28 h-1 (equivalent to 0.05 to 0.16 mL/min) at 60 bar, 250° C. Steady-state data were taken after 5 h on-stream, HAs represent organic acids containing-OH functional groups, and where varbon recovery: 80-88%.

[0103] FIG. **4***a* depicts the effect of temperature on product distribution over 0.25 wt % Pd/Nb2O5 at a constant WHSV of 2.85 h-1 and 60 bar pressure. At the lowest temperature (230° C.), gluconic acid conversion was high (90%), but 11% of the detected carbon products constituted acids with —OH functional groups (i.e., HAs). At higher temperatures, the selectivity to HA products decreases (FIG. **4***a*), suggesting favorable conversions of intermediate HAs such as glycolic and lactic acids. The selectivity to levulinic acid decreases with increasing temperature, indicating that levulinic acid is consumed via hydrogenation to GVL. The selectivity to carboxylic acids (which are ~90% acetic and propionic acids) decreases with increasing temperature. The pathway to ketones (mainly C6 cycloketones) is favored at higher temperatures. The presence of Nb2O5 has previously been reported to catalyze the ketonization of propionic acid to 3-pentanone.

[0104] FIG. **4***b* shows the effect of WHSV at a fixed temperature of 250° C. Longer contact time (1.43 h-1 WHSV) led to decreased selectivity to HAs and increased conversion of levulinic acid to GVL; however, the selectivity to esters decreased at the expense of hydrocarbon products (mainly 2-hexene). This could be attributed to the favorable decarboxylation of GVL under this condition to form butylene, which possibly undergoes conversion to 2-hexene. Furthermore, at the shortest contact time tested (4.28 h-1), the selectivity to HAs became significant. The only notable difference between the two pressures was the lower carbon recovery at 35 bar. At this condition, the pressure is insufficient to hold the gluconic acid in the aqueous phase, causing partial plugging of the reactor inlet. This is evinced by the observation of a brown-colored caky solid at the inlet resulting from gluconic acid crystallization.

Based on the above results, 250° C., 60 bar, and 2.85 h-1 was as a suitable baseline operating condition for subsequent experiments.

[0105] Eight representative organic acids were used to formulate a model mixture feed. This mixture approximates the complete set of organic acids separated from black liquor. These acids are divided into 9 classes based on the number of-COOH (1-2) and —OH (0-4) groups present. FIGS. **5***a* and **5***b* show the catalytic performance of 0.25% Pd/Nb2O5 for the hydrodeoxygenation of model mixed hydroxy acids at temperatures between 24° and 280° C. FIG. **5***a* depicts the conversion of individual hydroxy acids (gluconic acid (Gluc A), malic acid (MA), succinic acid (SA), glycolic acid (Glyc A), dimethylolpropionic acid DMPA, formic acid (Formic A), and Acetic Acid (Acetic A)), and FIG. **5***b* shows the product distribution. The data for longer contact time (i.e., 1.5 h-1 WHSV) at 260° C. are shown. Operating conditions: 60 bar, 50 mL/min H2 coflow, steady-state data were taken after 7 h on-stream, where carbon recovery: 78-82%.

[0106] FIGS. **5***a* and **5***b* depict the effect of temperature (240-280° C.) and WHSV at constant pressure (60 bar) and H2 flow (50 mL/min) on the conversion of each of the acids in the model mixture over 0.25% Pd/Nb2O5. Increased temperature increased the total conversion of HAs, suggesting faster reaction rates. The individual conversions of each acid also generally increased with temperature, but the acids showed a wide range of reactivity (FIG. **4***a*). At 260° C. and WHSV of 3.1 h-1, ~38% of lactic acid and ~43% of glycolic acid were converted. However, using these two molecules individually as reactants at comparable reaction conditions resulted in conversions of ~70% and ~48%, respectively, and widely different product distributions. This indicates other parallel reactions during the conversion of the 8-component mixture, leading to the production of lactic acid and hence a lower conversion. Similarly, no acetic acid conversion is seen in FIG. **5***a*, but a control experiment using 10 wt % acetic acid alone at 280° C./40 bar showed ~6% conversion on 0.25% Pd/Nb2O5. This suggests that acetic acid is converted to some extent in the mixture feed, but acetic acid formation via C—OH bond cleavages in the other acids also occurs. Thus, some components in the HA mixture feed can also appear as products of reactions of larger HAs.

[0107] The product distributions are shown in FIG. **5***b*. In general, the combined selectivity to oxygenated products decreased from 62% at 240° C. to 50% at 280° C., with the rest of the carbon detected in the product mixture being CO2 and hydrocarbons. At a constant WHSV of 3.1 h-1, higher temperature favored selectivity to carboxylic acids (C2-C6), from ~9% at 240° C. to 15% at 280° C., reaching 19% at longer contact times (1.5 h-1). Levulinic acid selectivity declined (and GVL selectivity increased) with increased temperature, suggesting that more levulinic acid was consumed on the catalyst sites to form GVL. Aromatics, anhydrides, and esters were observed to dominate at the lowest temperature, and their fraction decreased at higher temperatures. Two new species (isobutyraldehyde and isobutanol) were detected, probably due to the addition of C4-C5 HAs in the model mixed HA feed. These products were not detected during the conversion of gluconic acid, lactic acid, or glycolic acid alone. The selectivity for aldehydes (acetaldehyde and isobutyraldehyde) and alcohols increased with temperature. Aldehyde formation suggests decarboxylation via C—C bond cleavage on the Pd site with CO2 release. The aldehydes can form alcohols by direct hydrogenation, i.e., isobutyralde-hyde to isobutanol and acetaldehyde to ethanol (see, e.g., FIG. **2**). There is significant selectivity for COx (CO2 and CO) that increases with temperature (see, e.g., FIG. **5***b*). This can mainly be attributed to the decomposition of formic acid into H2 and CO2. Alternative pathways to CO2 during the hydrodeoxyge-nation process are also shown in FIG. **2**. The comparison of data from Pd/C and Pd/Nb2O5 in the HDO of model mixed HAs revealed that Pd/C is less active (47% versus 72% conversion) and generated significantly more CO2 than Pd/Nb2O5 at the same operating conditions. Meanwhile, 0.25 Pd/C offered a comparably superior selectivity to alcohols, levulinic acid, and aldehydes, probably due to the absence of catalytic sites to drive their further conversion during the HDO reactions. Finally, hydrocarbon products including light alkanes, light olefins, and 1-hexene/2-hexene were detected, with higher temperatures leading to higher hydrocarbon selectivity.

[0108] The organic acids making up the model mixture of HAs showed a wide range of reactivities on the niobia-supported Pd catalyst. Also, a strong correlation between reaction temperatures and product selectivity was observed. While low temperatures revealed selectivity to enols and esters, higher temperatures are selective to carboxylic acids, ketones, and aldehydes. Based on the finding that the presence of formic acid in the model HA mixture primarily determines the CO2/CO levels in the product stream, a good strategy to either utilize formic acid or control its production during the peeling reaction of carbohydrates in wood pulping is important. Overall, the partial HDO of mixed model acids revealed the importance of identifying a suitable combination of operating conditions (reaction temperature, pressure, WHSV, and H2 flow rate) to achieve an appropriate degree of hydro-deoxygenation and a more desirable product distribution for further upgrading.

[0109] The operating conditions determined from the conversion of the model acid feed were used as a starting point for HDO of the real HA mixture feed derived from kraft BL. This mixture (80 wt % acids) was diluted to ~8 wt % before use. The stability of the kraft BL-derived HAs was evaluated by catalyst-free control experiments conducted at 280° C. (the temperature used for converting the model acid feed) and at 330° C. The feedstock becomes increasingly unstable as the temperature increases, with ~25% conversion at 280° C. and ~38% conversion at 330° C. Carbon recovery decreased at the highest temperature tested. Gluco-isosaccharinic acid (GISA, ~25% in the HA feed) appeared the most sensitive to temperature. At 330° C., the oxygenates formed from the converted carbon species include volatile acids (mainly methacrylic acid), ketones (mainly acetone), acetaldehydes, alcohols, and esters. Based on these findings, as well as the optimum operating conditions in the HDO of mixed model HAs, a temperature range of 265-295° C. was chosen for further exploration. FIGS. **6***a* and **6***b* summarize the HDO of ~8 wt % aqueous HAs over 0.25% Pd/Nb2O5 at different temperatures (265, 280, and 295° C.), WHSVs (2.5 h-1 and 1.0 h-1), and at 60 bar pressure along with 50 mL/min H2 coflow. FIGS. **6***a* and **6***b* shown catalytic performance of 0.25% Pd/Nb2O5 for the hydrodeoxygenation of kraft BL-derived hydroxy acids, where FIG. **6***a* shows total HA conversion and product distribution at temperatures between 265 and 295° C. The data for longer contact time (i.e., 1.0 h-1 WHSV) at 280° C. are additionally shown. FIG. **6***b* shows reactor configuration for the catalytic conversion

of BL-derived HAs reported in this study, showing the major reactants and products. Operating conditions: 60 bar, 50 mL/min H2 coflow, the data were taken after 7 h on-stream, where carbon recovery: 66%-71%.

[0110] In the HDO step, the experiments were designed to completely remove the —OH functionality from the HA feedstock and produce a stream rich in a particular class of products (e.g., carboxylic acids, esters, or ketones). These are desirable for subsequent conversions to targeted chemical products, which will be the subject of future work. Due to favorable kinetics, the total conversion of HAs increases with temperature (FIG. **6***a*) at WHSV=2.5 h-1. Many of the acids comprising the BL-derived HA feedstock are temperature-sensitive, and their OH groups can be easily removed in the presence of 0.25% Pd/Nb2O5. However, glycolic acid, lactic acid, and 2,5-dihydroxypentanoic acid require further tuning of the operating conditions to achieve complete dehydroxylation. The total molar conversion of HAs increased from 45% at 265° C. to 86% at 295° C., indicating incomplete dehydroxylation. This can be attributed to the formation of 2-hydroxypentanoic acid as the HDO reaction proceeds. This intermediate HA could be formed from the partial C—OH cleavage of GISA. The latter is very temperature-sensitive, and a good correlation between its conversion and the formation of 2-hydroxypentanoic acid under all the conditions (including the control experiments) was observed. To achieve complete dehydroxylation, the residence time was increased by 60% (by loading more catalysts into the reactor and adjusting the H2/HA flow ratio) to obtain a lower WHSV of ~1.0 h-1. At 280° C. and 60 bar, H2 coflow of 45 mL/min, and WHSV of 1.0 h-1, complete cleavage of the alcohol C—OH bonds was achieved, corresponding to a total conversion of ~93% with the remaining 7% being acetic acid (FIG. **6***a*). At these conditions, a total of ~60% HDO of the feed stream was achieved, considering all oxygen present in the HA feed. FIG. **6***a* additionally depicts the distribution of liquid and vapor products during HDO of HAs at varying operating conditions. Generally, the selectivity to carboxylic acids (C3-C8) increases with temperature, while the selectivity toward ketones decreases. This is contrary to the trend in ketonic decarboxylation, which is favored at higher temperatures. This finding suggests that the main ketones found in the product are not necessarily the primary products of ketonization. The selectivity to aldehydes decreases with increasing temperature, at the expense of alcohols. Correspondingly, the selectivities toward CO2 and hydrocarbons (C1-C7) increase with temperature.

[0111] Table 2, shown below, includes the detailed product selectivities in the conversion of kraft BL-derived HAs over 0.25% Pd/Nb_2O_5 at 280° C., 60 bar, 1.0 h^{-1}, 50 mL/min H2 co-flow, corresponding to FIG. **6***a*.

TABLE 2

Group	Components	Carbon	mol %	Group	Components	Carbon	mol %
Carboxylic acids	Acetic	2	0.77	Ester	γ-valerolactone	5	1.01
	Propionic	3	25.10	Alcohols	Methanol	5	0.23
	n-butyric	4	3.85		Ethanol	2	0.09
	iso-butyric	4	17.42		Isobutanol	4	0.16
	2-methylbutyric	4	1.64		1-butanol	4	0.19
	Methacrylic	4	0.01		1-pentanol	5	0.15
	Pentanoic	5	11.17	COx	CO_2	1	17.42
	Hexanoic	6	0.63		CO	1	0.15
	4-methyloctanoic	8	0.64	Hydrocarbons	Methane	1	0.45
					Ethylene	2	0.92
Ketones	Acetone	3	2.33		1-Propylene	3	2.34
	Hydroxyacetone	3	0.01		1-Butene	4	1.33
	2-butanone	4	0.77		Pentane	5	0.37
	Methyl-cyclopentenolone	6	0.18		1-Pentene	5	0.01
	3 pentanone	5	0.99		2-Hexene	6	4.19
	4 heptanone	7	1.15		Hexane	6	0.76
	cyclohexanone	6	0.12		Heptane	7	0.02
	2-methyl cyclopentanone	6	0.13		Cyclohexane	6	0.02
	3-methyl cyclopentanone	6	0.11		Methyl Cyclohexane	7	0.21
Aldehydes	Acetaldehyde	2	0.18		Benzene	6	0.44
	Isobutyraldehyde	4	0.10		m-Xylene	6	0.17
Keto-acid	4-oxopentanoic acid	5	0.73		o-Xylene	6	0.32
					ethylbenzene		1.25
					Total		100

[0112] At the most suitable reaction conditions (280° C., 1.0 h-1), about 61% of the converted carbon is directed to C3-C8 carboxylic acid products, with propionic, n-butyric, i-butyric, and pentanoic acids comprising nearly all of this product class with very small amounts of hexanoic and 4-methyloctanoic acids. The high selectivity toward carboxylic acids is evident from the structural nature of the HAs in the feedstock, with >90% of the acids possessing an —OH functional group in their backbones, as well as the effectiveness of 0.25 wt % Pd/Nb2O5 in the selective cleavage of the C—OH bonds to form carboxylic acids. At reaction conditions unsuited for the complete dehydroxylation, increasing conversion of lactic and 2-dihydropentanoic acids led to a gradual increase in the selectivity to C3 and C5 carboxylic acids, indicating a correlation between the extent of conversion of these two HAs and the formation of C3/C5 carboxylic acids. Both HAs, though already present in the feed, are also generated during the reaction. At suitable

conditions, there is 6% selectivity toward several ketones. The 3-pentanone and 4-heptanone products are attributed to the primary ketonization products of C3 and C4 carboxylic acids on Nb2O5. Alternatively, 1-butanol can undergo ketonization to 4-heptanone. The formation of 2-butanone can be attributed to the decarboxylation of a keto acid (i.e., levulinic acid). Similarly, acetone could have formed via the decarboxylation of 3-oxobutanoic acid. However, this species was not observed in the GC/MS qualitative analysis, likely due to its instability. The aldehydes (1% of the product carbon) formed via decarboxylation reactions during C—C bond scission of HAscan undergo hydrogenation to alcohols. Alternatively, alcohols can be formed via direct hydrogenation of HAs, as is evident from the formation of 1-pentanol.

[0113] The steady-state vapor product analysis revealed that ~13% of converted carbon was directed to C1-C7 alkanes (2%), alkenes (8%), and aromatic (2%) hydrocarbons. It is noteworthy that the 2-hexene product was observed in the aqueous product stream, while all other reported products under the hydrocarbon group are in the vapor product. The formation of C2-C6 olefins can be attributed to different sources, including dehydration of alcohol over Nb2O5 acid sites, oligomerization reactions of C2 and C4 light olefins, or dimerization of propylene. In a prior study, decarboxylation of γ-valerolactone over niobia-containing catalysts released butylene as the main product. In a different investigation, the dimerization of propylene to hexene occurred at sufficiently high reaction temperatures (250° C.). Alkane formation can be attributed to the dehydration of alcohols followed by subsequent hydrogenation, while aromatic hydrocarbons from biomass feedstock have been previously attributed to stepwise cyclization, dehydrogenation, and aromatization reaction steps (e.g., as shown in FIG. **2**). The selectivity to COx reached ~18%, which is nearly all CO2 with a small amount of CO. Given this composition, separation of the hydrocarbons and other easily condensable gas/vapor products would allow for capture of a high-purity CO2 stream for storage or utilization. Finally, FIG. **6***b* shows a schematic summarizing the main product streams from the catalytic HDO of the BL-derived HA feed.

[0114] The steady-state data reported in FIG. **6***a* are taken at 7 h time-on-stream (TOS). To gain further insight into catalyst stability, extended conversion runs were performed at the suitable reaction conditions reported above. The transient data collected over 15 h TOS are depicted in FIGS. **7***a* and **7***b*. The normalized product distribution showed a steady increase in selectivity to C3-C8 acids in the first 4 h of the reaction, which was stabilized after 9 h. These TOS data suggest that the 0.25% Pd/Nb2O5 catalyst is stable under the current operation conditions. The powder XRD patterns of fresh and used catalyst samples show only a slight increase in pseudohexagonal Nb2O5 crystallite domain size from 12.2 nm (fresh) to 13.6 nm (used) based on the Scherrer equation. However, ~34% decrease in the BET surface area was observed by N2 physisorption analysis (see, e.g., Table 1).

[0115] The results from this study suggest that the mixture of hydroxy acids derived from kraft black liquor is a suitable mixture that may enable pathways to produce chemicals with a high market value. Upgrading the hydroxy acid stream to longer (C20 and higher) molecules could lead to higher-value products (e.g., biolubricants) that generate considerably more revenue compared to the current use of the hydroxy acids for combustion along with lignin to generate steam and electricity. As seen from the data in this experimental example, not all the carbon in the feed streams is recovered in the product streams (liquid and vapor). Although incomplete carbon balances are not uncommon in similar studies, it is worth reflecting on the likely causes of this mass balance nonclosure. These include loss of volatile products in the workup and transfer of samples after product collection, the presence of undetected light products, or the formation of heavy organic products that are trapped on the reactor walls, tubing, fittings, or catalyst surfaces. A potential solution in future studies could be to run the real HA feedstock with much higher concentrations (i.e., without dilution) to allow for substantial collection and analysis of heavy products. Furthermore, the pathways to the formation of hydroxy acids in BL are important in the context of catalytic conversion. While the content of cellulose in softwoods and hardwoods is similar, the hemicellulose in hardwood is typically greater, indicating that more hydroxy acids can be derived from hardwood than softwood. Thus, the hexoses, pentoses, and polysaccharides that determine the concentration of the hydroxy acids will vary with both wood type and cellulose/hemicellulose contents. Therefore, the HDO catalytic system must be designed to handle such variability.

[0116] In the context of catalytic upgrading of the mixture of HAs derived from kraft BL, the presence of formic and acetic acids is challenging. Formic acid is liberated during the peeling reaction, while acetic acid is formed via the hydrolysis of acetate groups of hemicellulose chains. The formation of these volatile acids is difficult to control during wood delignification, yet they are not particularly useful acids in complex, realistic HA mixtures from the perspective of efficient carbon utilization. This is especially so for formic acid, which gives off its carbon as CO2 during the HDO reactions. Thus, since both acids are commercially important intermediate chemicals, it may be more economically viable to isolate them from the HA mixture before catalytic processing. This way, the production of CO2 can be significantly minimized. Alternatively, the formic acid can be utilized via catalytic transfer hydrogenation as the source of hydrogen needed for the HDO reaction, without the need for an external supply of H2, but this would require tuning of the catalytic system. Although no significant Pd content was observed in the postreaction mixture that was accumulated for 10 h, there was evidence of loss from the solid catalyst after the reaction. Therefore, embodiments can be configured and adapted to minimize leaching.

[0117] The hydrodeoxygenation of a kraft BL-derived HA feedstock was demonstrated, specifically targeting the removal of-OH functional groups via C—OH bond scission on acid-assisted metal sites (bifunctional sites). The reactivity of gluconic acid, afforded by its carbon and OH numbers, made it a suitable model candidate to initially study the HDO behavior of HAs on supported metal catalysts. Initial catalyst screening revealed that Pd, Pt, Rh, and Ru supported on Nb2O5 are potentially effective for the HDO process; however, the 0.25% Pd/Nb2O5 catalyst showed superior performance in the extent of deoxygenation and selectivity to carboxylic acids, levulinic acid, and cyclic esters (GVL and gluconic acid lactones). The use of mixed model acids to approximate a real kraft BL-derived HA feed proved beneficial in understanding this complex/multicom-

ponent feedstock, where the concentration of formic acid in the feed was found to be the most significant contributor to the formation of CO2. In the final stage of this study, the kraft BL-derived HA feedstock containing at least 27 distinct HAs was successfully converted by HDO.

[0118] The catalytic studies of this experimental example revealed that 100% removal of OH functional groups can be achieved at 280° C., 60 bar, 1.0 h-1, and 50 mL/min H2 coflow. These conditions selectively produced a C3-C8 carboxylic-acid-rich product stream, showing that the HA mixture is a practical feedstock for producing a carboxylic-acid-rich product stream amenable to the synthesis of high-value chemicals and materials in subsequent reaction steps. Finally, the catalytic performance as a function of TOS showed the Pd/Nb2O5 catalyst with a nominal metal loading of 0.25 wt % gave good stability over 15 h of operation, without sacrificing the selectivity to desired products. In doing so, this work also demonstrates the crucial role of establishing optimum reaction conditions to drive catalytic HDO of complex mixtures such as HAs on bifunctional active sites.

Experimental Example 2—Recovery and Enrichment of Organic Acids from Kraft black Liquor by Simulated Moving Bed Adsorption

[0119] The C1-C6 organic acid fraction of kraft black liquor has potential as a valuable and high-volume biomass-derived molecular feedstock for the production of chemicals and materials. However, large-scale recovery and purification of the multi-component acid fraction are challenging. This experimental example presents the design and demonstration of a continuous simulated moving bed (SMB) adsorption process for the recovery and production of organic acids from kraft black liquor (BL). A combination of experimental multicomponent adsorption measurements, SMB operation, and model-guided process design was applied, using a granulated activated carbon adsorbent. The SMB modeling parameters, including adsorption isotherms and mass transfer parameters, were obtained experimentally through batch-mode and column breakthrough measurements using synthetic multicomponent acid streams. The preliminary SMB operating conditions were then determined by detailed SMB process modeling and optimization and fine-tuned experimentally with the aid of internal concentration profile measurements and heuristic principles of SMB operation. The adjusted operation condition was then validated by continuous production of acids with an actual pretreated BL stream. A high-quality organic acid mixture with 98% purity and 95% water rejection was obtained, with >85% acid recovery from the pretreated BL feed and a 4-fold increase in acid productivity per unit mass of adsorbent relative to a cyclic fixed-bed process. Approaches for managing the effects of residual lignin content in the pretreated feed are discussed.

[0120] Simulated moving bed (SMB) adsorption processes are known to offer better separation performance and cost-saving potential over cyclic fixed bed adsorption. SMB has broad industrial applications in the petrochemical, food, biochemical, pharmaceutical, and fine chemical industries. In a true moving bed (TMB) adsorption system, shown in FIG. **8***a*, solid (adsorbent) and liquid phases are circulated counter-currently, and the feed mixture is introduced in the center. The more-adsorbed species A (organic acids here) is carried by the solid adsorbent, moves leftward, and is then recovered by the liquid desorbent (C) to obtain the extract product. The less-adsorbed species B (water and inorganics here) mostly remains in the liquid, moves rightward, and is removed as raffinate. A conventional four-zone SMB, shown in FIG. **8***b*, has multiple fixed beds connected in a loop. To approximate the counter-current TMB, the four inlet/outlet ports switch simultaneously (synchronously) by one column length at each step. A full cycle has the same number of port-switching steps as the number of columns.

[0121] Model-guided SMB design is necessary as well as challenging. SMB performance is strongly dependent on the operating parameters, and multiple operating parameters must be determined and optimized in order to fall within the narrow parametric window of desired separation performance. In this experimental example, the model-guided design and experimental implementation of an SMB system for the recovery and enrichment of the organic acid fraction from a pretreated BL ("PBL"), obtained from a southeastern US softwood kraft mill is presented. First, the multicomponent adsorption thermodynamics and mass transfer parameters are determined with a synthetic (model) acid mixture via batch adsorption and fixed-bed breakthrough measurements. Next, a detailed system model-incorporating the adsorption model, mass transport between the solid and liquid phases, and motion of the fluid phases under synchronous switching conditions is used for accurate SMB simulations. Preliminary operating parameters (flow rates in each zone, switching time, and zone configuration) are predicted using the model and fine-tuned based upon experimental separation characteristics and the fundamental principles of SMB operation. A custom modification of the experimental SMB system described herein allows measurement of internal concentration profiles, thus allowing better tuning of system parameters. Finally, the experimental validation of the refined SMB operating conditions and the production of purified, concentrated organic acid mixtures from kraft BL is demonstrated.

Determination of Adsorption and SMB Parameters.

[0122] BL is a complex stream, and the acid fraction contains a large number of mono- and dicarboxylic acids with a range (0-4) of hydroxyl groups. The focus here is on recovering the entire acid mixture from BL, rather than specific acids. Initially, a synthetic feed stream containing only two representative acids was investigated. Glycolic acid (GA) and malic acid (MA) are selected to represent monocarboxylic acids and dicarboxylic acids in the BL stream. Four-component mixtures containing GA, MA, methanol (desorbent), and water are used for ad-sorption measurements, with water regarded as a non-adsorbing component on the hydrophobic GAC adsorbent. Multicomponent adsorption isotherm parameters were obtained for this four-component system using batch adsorption at 295 K. After testing several multicomponent isotherms, including multicomponent Langmuir (ML), mixed linear and Langmuir (MLL), and extended Sips isotherms, the competitive MLL model is selected to fit multicomponent adsorption data:

$$q_i = H_i c_i + \frac{q_{s,i} K_i c_i}{1 + \sum K_i c_i},$$

where, $q_{s,i}$ and K_i are the saturation uptakes and Langmuir constants, and H_i is the Henry's constant of species i. This isotherm was chosen given its better accuracy compared to the other two multicomponent isotherms and its ability to describe selective adsorption that occurs in the adsorbent at the micropores with the competitive Langmuir term, as well as the nonselective pore-filling adsorption that occurs at the larger pores with the linear term.

[0123] Due to the significant presence of micropores (<2 nm), mesopores (2-50 nm), and macropores (>50 nm) in GAC adsorbent, the transport dispersive model (TDM) is used to describe the fixed bed breakthrough. The TDM incorporates the component concentration at three levels: the bulk liquid, the meso/macropores, and the adsorbed phase (which is largely microporous), and thus is well suited for this type of hierarchical pore structure. The values of the mass transfer coefficients $k_{app,i}$ are obtained after fitting experimental breakthrough curves to the model using a sum-of-squared-errors criterion. The fitted isotherm and mass transfer coefficients are shown in Table 3 below.

TABLE 3

Components	H (cc/g GAC)	q_s (g/g GAC)	K (cc/g)	k_{app} (1/min)	Density (g/cc)	Weight fraction
GA	0.61	0.084	254	0.8	1.5	2.47%
MA	0.52	0.117	1208	1.22	1.6	0.11%
Water	0.001	0.001	0.001	1.0	1.0	97.42%
Methanol	0.06	0.049	79	0.69	0.79	0

[0124] A four-zone, eight-column SMB system with a 2-2-2-2 zone configuration (see, e.g., FIG. **8***b*) is used in this work. The bed and particle porosities are determined by the textural characterization of the GAC adsorbent. These parameters are listed in Table 4 below.

TABLE 4

System parameter	Value
# of Columns	8
Zone Configuration	2-2-2-2
Column length (cm)	20
Column inner diameter (cm)	1
GAC loading per column (g)	6.3
Bed porosity ε_b	0.44
Particle porosity ε_p	0.66

[0125] Using the parameters obtained in Tables 3 and 4, the initial SMB operating condition at 295 K was determined by employing robust modeling and optimization techniques. The mathematical model was formulated similar to the work of Chiang et al., wherein the convection-diffusion equation is used to describe the mass balance of the bulk fluid phase and the linear driving force model is used to represent mass transfer into the particle. (See, for example, Chiang et al. "Separation and purification of furans from n-butanol by zeolitic imidazole frameworks: multi-component adsorption behavior and simulated moving bed process design," ACS Sustain. Chem. Eng. 2019, 7 (19), 16560-16568; and Chiang et al. "Separation and purification of 2,5-dimethylfuran: process design and comparative techno-economic and sustainability evaluation of simulated moving bed adsorption and conventional distillation," ACS Sustain. Chem. Eng. 2020, 8 (33), 12482-12492, both documents are incorporated herein by reference in their entirety). The objective function of the optimization problem is to minimize desorbent consumption, subject to the separation performance specifications. The mathematical problem was formulated as a system of partial differential algebraic equations using Pyomo.DAE and solved using sIPOPT 3.13.1. The performance specifications are >90 wt % acid content in the desorbent-free (D-free) extract, and >90% recovery (by mass) of acids from the feed. The resulting SMB operating condition prediction is regarded as the preliminary SMB design (e.g., as shown in Table 5 below), and the operation variables are described in the table caption. Based on this prediction, the first SMB experiment (run #1) was carried out on a two-acid synthetic feed stream. After the SMB system reaches cyclic steady state (CSS), the extract stream is collected throughout a full cycle and then analyzed. The experimental results are compared with the model prediction in Table 6. As can be seen from the results of run #1, the preliminary model overestimated both the acid content and recovery in the extract, indicating the need for further accuracy in the determination of the system parameters. To obtain additional experimental information beyond the product compositions, we implemented a modification of the SMB system by installing a sampling device for measuring the fluid compositions in each column just before the port switching (the end of the step), after CSS was reached.

[0126] Table 5 shows SMB operating conditions from the model, and those corresponding to the experimental runs. Percentages in parentheses (Runs #2-#4) show the extent of the intentional operation adjustments relative to Run #1. The operational variables are defined as follows: FD is the methanol desorbent flow rate, FExt is the extract flow rate, FFd is the feed flow rate, FIII is the Zone III flow rate, t_switch is the step time for port switching.

TABLE 5

Operating Parameters	Preliminary Design	Run #1	Run #2	Run #3	Run #4
F_D (cc/min)	1.17	1.29	1.30	1.27	1.30
F_{Ext} (cc/min)	0.95	0.91	0.91	0.90	0.93
F_{Fd} (cc/min)	2.00	2.00	1.79 (−10%)	1.60 (−20%)	1.63 (−19%)
F_{III} (cc/min)	3.37	3.39	3.18 (−6%)	3.00 (−12%)	3.00 (−12%)
t_switch (min)	10.0	10.0	9.5 (−5%)	9.1 (−9%)	9.4 (−6%)

Table 6 shows the experimental separation performance of the SMB using two-acid synthetic streams (model-predicted performance in parentheses).

TABLE 6

Run No.	% Acid Recovery in Extract	wt % Acids in D-free Extract	Water removal %
Run #1	66 (86)	43 (94)	96 (100)
Run #2	90 (90)	29 (73)	94 (99)
Run #3	90 (88)	11 (48)	78 (97)
Run #4	95 (90)	26 (56)	93 (98)

[0127] The experimental fluid-phase concentration profiles of the four components (GA, MA, methanol, and water) for run #1 are compared with the model predictions in FIG. **9**. The model captures most of the features of the actual profiles. However, at the position where the extract is collected, the model slightly overestimates the acid content but largely underestimates the water content. Therefore, both acid content and recovery are overestimated in the extract. Also, water is much more abundant than acids in the feed, and even small deviations in the water concentration predictions can have a significant effect on the acid recovery and acid content in the extract. There are several possible reasons for the deviation between the calculated and experimental concentration profiles. The adsorption isotherms for water may not be accurate enough. Also, it was assumed that the rate-limiting step is the mass transfer between the bulk liquid and the meso/macropores and that the mass transfer resistance between the meso/macropores and the adsorbed phase is negligible. This assumption might not be suitable for water, which has a high concentration in the fluid phase but is very lowly concentrated in the hydrophobic adsorbed phase. Cross-contamination due to the system dead volume (e.g., tubing and valves) can be another reason since back-mixing is not considered in the model. The dead volume contribution can horizontally shift the profile of a poorly adsorbed component by a considerable amount. Although the system dead volume is only ~3% of the total bed volume, in the case of water (present in high concentration), even a small shift can lead to inaccurate predictions.

Adjustment of SMB Operating Conditions.

[0128] Starting from the insights obtained in run #1 (the initial SMB experiment), the SMB performance was improved by fine-tuning one or two operating parameters in each subsequent experimental trial with the two-acid synthetic feed (such as shown in Table 5). Additional simulations were performed with these adjusted operation parameters to qualitatively verify the expected improvement in separation performance. To improve the acid recovery in the extract stream, the loss of acids in the raffinate stream needs to be reduced, which can be achieved by reducing the switching time (i.e., more frequent switching).

[0129] This can be understood by the analogy between the SMB and TMB in FIGS. **8***a* and **8***b*. A reduction of SMB switching time is equivalent to a faster TMB counter-current motion in FIG. **8***a* so that the strongly adsorbed species (acids) can be carried more efficiently to the extract side, which leads to a lower content of remaining acids in the raffinate. However, the switching time must not be too small, such that the solid velocity becomes too large compared to the fluid velocity, thus making the desorption step in zone I inefficient. Furthermore, the feed mixture is introduced between zones II and III. To improve the acid recovery in the extract, more acids need to be transferred to zone II from zone III. This can be achieved by reducing the liquid flow rate in zone III so that acids can be carried more efficiently to zone II by the moving solid phase. By reducing both feed and raffinate flow rates, zone III flow rates can be decreased while keeping the flow rates in all the other three zones unchanged.

[0130] With reference now to FIG. **10**, FIG. **10** shows the internal concentration profiles collected from run #2, shown in FIG. **10***a*, run #3, shown in FIG. **10***b*, and run #4, shown in FIG. **10***c*, which are indicated by a solid curve with closed dots. They are compared with those in run #1 (initial SMB experiment), which are shown in a dashed curve with open dots. For a clear comparison, the methanol profile is removed, the summation of GA and MA content is calculated as total acid content, and the y-axis is in log scale. Based on the above observations, the switching time and zone III flow rate are reduced in run #2 by 5 and 6%, respectively (Table 5) relative to run #1. The internal concentration profile of run #2 is shown in FIG. **10***a*. As expected, the acid profile in zone III moves toward the extract to a larger extent compared to run #1. The acid content at the raffinate position is significantly decreased. The acid profile in zone I also moves slightly leftward, leading to a slightly increasing acid content at the extract position. The resulting separation performance is shown in Table 6. The acid recovery in the extract increases to 90%. However, the acid content in the D-free extract dropped significantly to 29% as the water profile also moved toward the extract. A trade-off between acid recovery and water removal exists.

[0131] To determine whether the acid recovery can be further improved, switching time and zone III flow rate are further reduced in run #3 (Table 5). However, the recovery does not increase further while the purity is significantly reduced (Table 6). In FIG. **10***b*, both acid and water profiles move leftward within zones I to III compared to run #1. The water content is significantly higher at the extract port, but the absolute acid content does not change significantly compared to run #1, which leads to the sharp decrease of the acid content in the D-free extract. On the other hand, the acid content is significantly higher in zone I when compared to run #1 due to the shorter switching time. When port switching is too fast, it is equivalent to fast solid movement and recycle shown in FIG. **8***a*. If the content of the more retained species (acids) is too high in zone I, as seen in FIG. **10***b*, the solid circulation loop can carry it to zone IV. Then, it can travel further leftward and contaminate the raffinate stream, which leads to the loss of the adsorbed species in the raffinate. Therefore, reducing switching time or accelerating solid movement to improve acid recovery is only effective in a certain range of operating conditions. Accordingly, in run #4, the zone III flow rate is kept the same as in run #2, while the port switching is slower in run #4 when compared to run #3. The resulting acid and water profiles in run #4 (FIG. **10***c*) are similar to those in run #2, but with lower acid content at the raffinate port that reduces the loss of acids in the raffinate stream. Both acid content and recovery in the D-free extract are increased when compared to run #3, and the 95% acid recovery is the highest among the four SMB operations. At this point, it became apparent that the acid content (wt % in

the D-free extract) criterion is too stringent and should be replaced by an equivalent water rejection criterion, i.e., the % of water in feed that is rejected into the raffinate. In the case of run #4, the acid content in D-free extract is 26%, which is equivalent to 93% water removal/rejection. After water removal reaches 90% (corresponding to ~22 wt % enriched acid extract), the water removal increases very slowly with increasing acid content in D-free extract. Overall, the operating condition of run #4 leads to 95% acid recovery and 93% water removal, which is a viable separation process. As seen from Table 6 for all four SMB experiments, the model prediction of acid recovery is quite good, indicating accurate calculation of acid adsorption and transport in the SMB system. The large deviation in the acid content prediction is due to the difficulty in accurately modeling the water profile and is caused by the high concentration of water and a lack of knowledge of water adsorption in the micropores (it is assumed that water can fill the macro/mesopores but is nonadsorbing in the hydrophobic micropores). These factors could be targets of a more detailed future investigation.

Validation of Operating Conditions.

[0132] Due to the efficient recovery of acids from the two-acid synthetic feed stream in run #4, further validation was investigated using a more complex acid-aqueous mixture with the same operating conditions before proceeding to actual BL streams. A synthetic feed stream of eight representative acids plus Na2SO4 was formulated to simulate different classes of organic acids (determined by the amount of —COOH and —OH groups) in the PBL. The concentration of each representative acid is set to match the total acid concentration of the corresponding acid class in the PBL stream. Na2SO4 is the predominant inorganic salt in the PBL and is thus included as the only inorganic component in the synthetic feed stream. The operating condition of run #4 was validated with the detailed synthetic feed stream (2.6% total acids and 0.7% salt) in a 30 h SMB run. The D-free composition of the two outlet streams, extract and raffinate, was measured periodically and is shown in FIGS. **11***a* and **11***b*. The CSS is reached after 7 cycles (around 9 h). At steady-state, the D-free extract contains 27 wt % acids (corresponding to 91% acid recovery and 92% water removal/rejection), while the salt content (<0.2 wt %) is significantly lower than the feed stream, thus confirming successful separation of acids from water and inorganic salt. The D-free raffinate is almost pure (99%) water with 0.8% Na2SO4 and only 0.2% acids.

[0133] The average SMB separation performance during 9-30 h after SMB starts (i.e., after CSS) is summarized in the first entry of Table 7 (shown below), and the compositions of the outlet streams are shown in the top half of Table 8 (shown below). Table 7 shows the average separation performance of the SMB run over 20 h after onset of CSS using the detailed synthetic stream and actual PBL as the feed stream and Table 8 shows composition of inlet and average composition of the outlet streams during the last 20 h from SMB unit using the detailed synthetic stream and actual PBL as the feed stream.

TABLE 7

Feed Stream	Rec $\%_{Acids,\ Ext}$	Remv $\%_{Water}$	Pur $\%_{Acids,\ Ext}$
Detailed synthetic stream	91	92	/
Actual PBL	86	95	98

TABLE 8

SMB #	Components	Before pretreatment	Feed for SMB	D-free Extract	D-free Raffinate
Multicomponent Synthetic Feed	Acids (wt %)	N/A	2.6	27.0	0.2
	Salts (wt %)	N/A	0.7	0.2	0.8
	Water (wt %)	N/A	96.7	72.8	99.0
Kraft Black Liquor	Acids (wt %)	2.6	2.6	36.8	0.4
	Salts (wt %)	8.6	0.8	0.3	0.8
	Lignin (wt %)	5.6	0.03	0.1	0.0
	Water (wt %)	83.2	96.6	62.8	98.8

[0134] The acid content in the D-free extract and the water removal are very similar to those obtained from the two-acid feed and indicate that the GAC adsorbent is strongly selective for organic acids. The slight changes in performance between the two feeds can be attributed to the quantitative difference in adsorption and diffusion behavior of the acids present in the two feeds. The internal concentration profile was also collected after CSS was reached, e.g., as shown in FIG. **12**, where FIG. **12** depicts the measured internal concentration profile from SMB steady-state operation with multicomponent synthetic feed. Individual acid profiles are marked with open symbols, and the total acid profile (sum of the individual acid profiles) is marked with closed symbols. They-axis is on a logarithmic scale. The total acid profile is almost the same as in FIG. **10***c*. The profiles for individual acids show a similar pattern, indicating strong adsorption in the GAC adsorbent in all cases. The water profile is also similar to that of the two-acid synthetic feed stream. The Na2SO4 salt profile closely tracks the water profile, showing the effective rejection of both species from the extract. After validation with the multicomponent synthetic feed stream, the same SMB operating condition was applied to the actual PBL stream with another 30 h run. Besides 25.8 g/L acids, the other significant component is 7.7 g/L Na2SO4. Additionally, some trace/residual lignin (0.3 g/L) remains in the PBL feed.

[0135] The composition profiles of D-free extract and raffinate are shown in FIGS. **13***a* and **13***b*. In FIGS. **13***a* and **13***b*, the composition of D-free extract (FIG. **13***a*) and raffinate (FIG. **13***b*) using actual PBL as a feed stream over a 30 h SMB run is shown, where the feed compositions are denoted by dashed lines, and the y-axis is on the log scale. As expected, the acid mixture is enriched in D-free. The major components in the D-free extract and raffinate (acids, Na2SO4, and water) reach CSS in a manner similar to the synthetic feed stream. However, residual lignin requires a much longer time to approach CSS. This is expected because lignin is a stronger-adsorbing component than the acids, a fact which motivates lignin removal in the pretreatment of the kraft BL before acid recovery. More lignin is withdrawn from the extract, and the lignin content in D-free extract gradually exceeds feed concentration as lignin is a strong adsorbing component on GAC. Furthermore, the combined outlet mass flow of lignin (in extract+raffinate) is lower than the inlet mass flow (in feed), showing that some of the

residual lignin slowly accumulates in the adsorbent. The SMB performance over the run is summarized in FIG. **14**, which depicts separation performance summary with the real PBL as the feed stream over a 30 h SMB run. The average SMB separation performance in the 9-30 h interval (in which the compositions of the major components reach CSS) is summarized in Table 7, and the composition of the outlet streams is shown in Table 8. The acid content in the D-free extract is 37% with 95% water rejection from the feed stream, compared to 27% D-free extract acid content and 92% water rejection with the multicomponent synthetic feed. Thus, the extract quality and water rejection are considerably better than those obtained with the complex synthetic feed. In the case of the PBL feed, water must compete for adsorption sites not only with the organic acids but also with lignin, a more strongly adsorbing species. The result is higher water rejection and a more concentrated acid product. On the other hand, due to the occupation of some adsorption sites by lignin, the acid adsorption capacity is lower, resulting in 86% acid recovery (lower than the 91% acid recovery from the synthetic feed). Lignin has a larger molecular size and hence slower diffusion in the GAC pores, resulting in a slow approach to equilibrium adsorption (or CSS in the case of SMB, as seen in FIGS. **13***a* and **13***b*).

[0136] Table 9 shown below summarizes the performance of the present continuous SMB adsorption process compared to that of a cyclic fixed bed adsorption process from our recent work (see, e.g., Fu, et al. "Recovery and enrichment of organic acids from kraft black liquor by an adsorption-based process," ACS Sustain. Chem. Eng. 2022, 10 (34), 11165-11175., incorporated by reference herein in its entirety), where *purity refers to the percentage of acids in the total dissolved solids (acids, salt, and lignin).

TABLE 9

	Productivity (kg Acids · ton $GAC^{-1} \cdot hr^{-1}$)	D/F Ratio	% Acids Recovery in Extract	% Water Rejection	% Purity Acids in D-free Extract*
SMB (this work)	43	0.8	86	95	98
Cyclic fixed-bed[15]	11	2.5	92	79	95

[0137] It is clear that SMB removes much more water from the PBL stream and produces an enriched acid mixture with higher purity. Due to the countercurrent operation, SMB is more efficient and uses much less desorbent than fixed bed operations, as shown by the desorbent-to-feed ratio (D/F). Table 9 also shows nearly 4-fold higher productivity (43 kg of acids produced per ton of GAC per h) of the SMB, which is in the same range as industrially feasible large-scale SMB processes for petrochemical and sugar production. While the cyclic fixed-bed process can also be further optimized, the large advantages in productivity and low desorbent use in SMB appear difficult to reproduce in a fixed-bed process.

[0138] FIG. **15** compares the molecular weight distributions (MWDs) of lignin in the kraft BL, partially delignified BL (NF permeate), and highly delignified ("lignin-free") PBL, which is the pretreated feed stream to the SMB. The NF membrane greatly reduces the lignin content of the BL, especially that of HMW lignin with MW >2000. Further adsorption pretreatment using the GAC adsorbent removes nearly all the LMW lignin fragments present in NF permeate since they can adsorb strongly in the GAC micropores. However, a small amount of residual lignin (~0.3 g/L, as mentioned earlier) is still present in the PBL, with intermediate MWs in the "transition" range between LMW and HMW. In this region of MW, neither the membrane NF nor the GAC adsorbent pretreatment is optimally effective. While the present SMB process provides a high degree of acid enrichment and acid recovery from PBL, one option to further reduce lignin could be to select NF membranes with a tighter MW cutoff (MWCO) that can remove the intermediate-MW lignin along with the HMW lignin. Alternatively, the GAC adsorbent for pretreatment could be selected (or modified) to have a broader micropore distribution that allows adsorption of the intermediate-MW lignin along with the LMW lignin. Irrespective of the potential modifications in the pretreatment processes, another option-mentioned earlier in this paper-is to improve the SMB model in future work so that operating conditions can be optimized rigorously to obtain acceptable extract streams while also allowing more effective desorption of the lignin. In particular, accurate modeling of water in the SMB and the inclusion of residual lignin adsorption and mass transfer characteristics would be desirable. The SMB model parameters can also be further tuned by fitting them to the experimental SMB results. Embodiments of the present disclosure provide scaled-up design and demonstration of organic acid recovery and enrichment from BL streams were achieved on a continuous SMB system by developing and applying a combined experimental and model-guided process design approach. This approach allows accurate predictions of the behavior of acids and other BL components in the SMB system, thereby enabling identification of candidate operation conditions for the SMB, which could then be adjusted further by variations in experimental SMB operation aided by heuristic principles of SMB operation. At the same time, future challenges and opportunities in accurate modeling of water and management of residual lignin during the pretreatment of the BL feed stream toward a fully model-guided design and operation of such processes were identified. Despite the challenging nature of the multicomponent BL stream, the embodiments of the process shown and described herein (e.g., process **100**) produces promising results: an enriched acid feedstock mixture of excellent quality (98% acid purity, 95% water removal) with a high (86%) recovery from the PBL feed. The unique composition of this molecular biomass-derived feedstock is of considerable interest in the production of higher-value chemicals and materials.

[0139] Furthermore, embodiments of the process design (e.g., as detailed in FIGS. **1***a* to **1***c*) can be configured and adapted for integration with existing kraft processes to maintain a closed loop of water and chemical usage. A significant challenge in extracting valuable feedstocks from weak black liquor lies in the lack of cost-effective separation technologies that can be seamlessly integrated into the traditional kraft process without disrupting its core operations. The kraft chemical recovery cycle, a mature technology refined over decades, efficiently recovers pulping chemicals as white liquor and generates steam for drying pulp and paper by burning concentrated black liquor. Thus, embodiments of the process shown and described herein ensures economic viability by recycling pulping chemicals and energy, making kraft pulp and paper production highly

competitive. Accordingly, integrating embodiment of the novel bio-product recovery technologies into the kraft process must align with its foundational principle: preserving chemical and energy recovery to maintain its economic advantage.

[0140] Embodiments of the integrated process can provide, at least, the following advantages: enhanced economic efficiency of the kraft process, including (1) reduction of energy consumption in concentrating wBL total solids (TS) from 15% to 30%; (2) recovery of organic acids for valorization into high-value products; (3) recovery of pulping chemicals (e.g., NaOH, Na2S) to sustain kraft operations; (4) water recovery for process reuse; and (5) CO_2 recovery to support decarbonization goals.

[0141] FIG. **16** shows normalized concentration profiles of outlet streams from cycle #8 and #9 of cyclic fixed-bed adsorption 23 cycles to assess the long-term separation performance of GAC over 23 cycles. The color-coded areas with green, blue, and orange represent adsorption, desorption, and washing steps, respectively. The outlet stream of desorption step is collected as extract while the outlet stream of wash 1, adsorption, and wash 2 steps are collected as raffinate. As illustrated in FIG. **16**, no salt precipitation was observed: (1) between adsorption and desorption steps, as the salt concentration was diluted below its solubility limit before introducing the desorbent; and (2) between desorption and adsorption steps, as the wash 2 step effectively displaced the desorbent in macropores and micropores of GAC, preventing salt precipitation before feed was reintroduced. Salt precipitation could hinder the diffusion of organic acids into pores, resulting in a reduced adsorption rate. The GAC column demonstrated stable separation performance, achieving average recovery of 81% lignin, 68% organic acids, 27% water, 9% Na2SO4 in the extract, as shown in FIG. **16**. The raffinate, consisting of the acidified permeate and washing water, recovered an average of 90% of the salt, 70% of water, and only 30% of acids and 20% of lignin. Thus, the feed is effectively a purified stream of mainly salt (~30 g/L) and water with low lignin concentration (~0.42 g/L) which is important to prevent membrane fouling for downstream bipolar membrane electrodialyzer.

[0142] The production of organic acids presents an additional profit opportunity for pulp plants, serving as renewable feedstocks for lubricant production30. Although the acids are concentrated to 43 g/L, representing a 1.5 fold increase to the feed's acid concentration, further scale-up to continuous simulated moving-beds and process optimization could help reduce water content in the extract and increase acids recovery to 85% and purity to 98%, as achieved in our previous work. FIGS. **17***a*-**17***d* show recovery of lignin, acids, Na2SO4, and water to extract (FIG. **17***a*) and raffinate (FIG. **17***b*) and desorbent-free concentration profiles of extract (FIG. **17***c*) and raffinate (FIG. **17***d*) streams over 23 cycles. With further optimization of adsorbents and process, embodiments of the integrated kraft process have the potential to become more sustainable by recovering more organic acids with reduced desorbent and energy consumption as compared to conventional kraft process.

[0143] Additional technical details of potential embodiments are provided in the attached appendices. In particular, any of the embodiments described herein can further include one or more steps or components disclosed in the appendices. However, the appendices should not be construed to limit the scope of the above disclosure or the claims that follow.

[0144] It is to be understood that the embodiments and claims disclosed herein are not limited in their application to the details of construction and arrangement of the components set forth in the description and illustrated in the drawings. Rather, the description and the drawings provide examples of the embodiments envisioned. The embodiments and claims disclosed herein are further capable of other embodiments and of being practiced and carried out in various ways. Also, it is to be understood that the phraseology and terminology employed herein are for the purposes of description and should not be regarded as limiting the claims.

[0145] Accordingly, those skilled in the art will appreciate that the conception upon which the application and claims are based may be readily utilized as a basis for the design of other structures, methods, and systems for carrying out the several purposes of the embodiments and claims presented in this application. It is important, therefore, that the claims be regarded as including such equivalent constructions.

[0146] Furthermore, the purpose of the foregoing Abstract is to enable the United States Patent and Trademark Office and the public generally, and especially including the practitioners in the art who are not familiar with patent and legal terms or phraseology, to determine quickly from a cursory inspection the nature and essence of the technical disclosure of the application. The Abstract is neither intended to define the claims of the application, nor is it intended to be limiting to the scope of the claims in any way.

What is claimed is:

1. A process for obtaining new products from a kraft mill and for improving operational efficiency of a kraft mill through extraction of bioderived organic acids and liquid CO_2 from weak black liquor generated during a kraft process, comprising the steps of:

filtering a weak black liquor (BL) stream generated in the kraft process downstream from a brownstock washer to remove a first portion of lignin and generate a reduced lignin or delignified permeate and a retentate;

removing the reduced lignin or de-lignified permeate from the kraft process;

processing at least the de-lignified permeate to generate organic acids, liquid CO_2, water, and raffinate containing salts;

recovering the organic acids, and liquid CO_2; and

returning the raffinate containing salts to the kraft process downstream of a recovery boiler.

2. The process of claim **1**, further comprising the step of, allowing the retentate of the filtered weak BL stream to remain within the kraft process.

3. The process of claim **1**, wherein the processing step further comprises the steps of, passing the reduced lignin or de-lignified permeate through a gas bubbler to generate an aqueous stream and a gas stream;

passing the aqueous stream through an adsorption column to remove a second portion of lignin from the reduced lignin permeate to generate a delignified BL stream;

passing the delignified BL stream to a crystallizer to precipitate at least a portion of salt in the delignified BL stream to generate a pretreated BL stream.

4. The process of claim **3**, wherein the processing step further comprises the steps of:

passing the gas stream to a liquifying unit configured to liquify the gas stream to liquid CO_2 and storing the liquid CO_2.

5. The process of claim **3**, further comprising the step of regenerating the adsorption column with an acetone-water mixture.

6. The process of claim **5**, wherein the processing step further comprises the steps of:

removing, at least a portion of organic acids in the pretreated BL stream to generate a reduced-acid or acid-lean pretreated BL stream and converting the organic acids to one or more organic chemicals; and

passing the reduced-acid pretreated BL stream through a reverse-osmosis membrane to generate the water and the raffinate containing salts.

7. A method of obtaining components from a kraft black liquor feedstock, comprising:

passing a BL feedstock through a NF membrane to remove a first portion of lignin in the BL feedstock to generate a NF permeate;

acidifying, with an acidification unit, the NF permeate to generate an aqueous stream and an off-gas stream including CO_2;

filtering, with a filtration unit, the aqueous stream to remove a second portion of lignin from the aqueous stream to generate a delignified BL stream;

removing, at least a portion of organic acids in the pretreated BL stream to generate a reduced-acid pretreated BL stream and a recovered organic acid stream;

passing the reduced-acid pretreated BL stream through a membrane to generate a water permeate and a raffinate comprising salt and recovering the water permeate;

passing the raffinate comprising salt through a membrane electrolyzer to generate an acidic stream and a basic stream; and

liquifying gaseous CO_2 from within the off-gas stream into a liquified CO_2 stream and recovering the liquified CO_2 stream.

8. The method of claim **7**, wherein the membrane electrolyzer is a Bipolar Membrane Electrodialyzer (BMED).

9. The method of claim **7**, further comprising causing one or more reactions between the at least a portion of the organic acids from the recovered organic acid stream and one or more catalysts to produce organic chemicals.

10. The method of claim **9**, wherein the one or more reactions comprise one or more reactions selected from the group consisting of deoxygenation, dehydroxylation, and oligomerization.

11. The method of claim **7**, wherein the NF membrane is an alkali-stable NF membrane.

12. The method of claim **7**, wherein the first portion of lignin in the BL feedstock comprises at least 93% of lignin in the BL feedstock.

13. The method of claim **7**, wherein the filtration unit includes a filter and the aqueous stream passing though the filter has a pH of at least 11.

14. The method of claim **7**, wherein the second portion of lignin from the NF permeate comprises at least 3% of lignin in the BL feedstock.

15. The method of claim **7**, wherein passing the BL feedstock through a NF membrane further comprises, separating the NF permeate from a retentate, and wherein the BL feedstock is taken from a kraft process and the NF permeate is processed outside of the kraft process and wherein the retentate is returned to the kraft process.

16. The method of claim **7**, wherein the acidifying step includes acidifying the NF permeate with H_2SO_4 to generate the aqueous stream and wherein the off-gas stream includes H_2S, SO_2, and CO_2.

17. The method of claim **16**, further comprising scrubbing the off-gas stream with a gas scrubber, wherein scrubbing includes introducing the off-gas stream and the basic stream into the gas scrubber, and generating the gaseous CO_2 stream.

18. The method of claim **7**, wherein the removing step includes removing organic acids from the pretreated BL stream with a simulated-moving bed unit, wherein the simulated-moving bed removes at least 90% of organic acids in the pretreated BL stream.

19. The method of claim **18**, wherein the simulated-moving bed utilizes a methanol or acetone desorbent.

* * * * *